Supporting Information

β-Lactonization of fluorinated porphyrin enhances LDL binding affinity, cellular uptake with selective intracellular localization

Juan Tang,[a] Juan-Juan Chen,[a] Jing Jing,[a] Jia-Zhen Chen,[a] Hongbin Lv,[a] Yi Yu,[a] Pingyong Xu,[b] Jun-Long Zhang*[a]

[1] Beijing National Laboratory for Molecular Sciences, State Key Laboratory of Rare Earth Materials Chemistry and Applications, College of Chemistry and Molecular Engineering, Peking University, Beijing, P.R. China

[2]National Laboratory of Biomacromolecules, Institute of Biophysics, Chinese Academy of Sciences, Beijing, P. R. China

*To whom corresponding should be addressed.

E-mail: zhangjunlong@pku.edu.cn

Table of Contents

1. Experimental Section

1.1 General experimental information

Commercially available chemical reagents, solvents, and silica gel were used without further purification. LysoSensor™Yellow/Blue DND-160, ER-Tracker Green, MitoTracker Green FM, Lipfectamine™ 2000 and Hoechst 33342 were purchased from Invitrogen (Carlsbad, CA, USA). The apoptosis detection kit with annexin V-FITC and propidium iodide was purchased from Beyotime Institute of Biotechnology (China). The ^{1}H and ^{19}F NMR spectroscopic measurements were performed using a Varian 300 NMR spectrometer with internal reference: ^{1}H (referenced to TMS at δ = 0.0 ppm) and ^{19}F (referenced to hexafluorobenzene (C_6F_6) at δ = 0.0 ppm). Chemical shifts of ^{1}H and ^{19}F spectra were interpreted with the support of CS ChemDraw Ultra version 11.0. Electrospray ionization (ESI) mass spectra were recorded on a Fourier Transform Ion Cyclotron Resonance Mass Spectrometer (Bruker, USA). The UV-*vis* absorption spectra were obtained with an Agilent 8453 UV-*vis* spectrophotometer in 10 mm path length quartz cuvettes. Single-photon luminescence spectra were recorded using an Edinburgh Instrument FLS920 Fluorescence Lifetime and Steady state spectrophotometer. Confocal fluorescent microscopy of living cells was performed using Olympus LSCMFV500 scanning laser microscope and Nikon A1R-si Laser Scanning Confocal Microscope (Japan). Flow cytometrical analysis was using a FACS Calibure or FACS Aria Ⅱ flow cytometer (BD, USA). All measurements were performed at room temperature.

1.2 Extinction coefficients and fluorescence quantum yield determination

Extinction coefficients were obtained from absorbance of Soret and Q bands versus the concentrations. Corrected emission spectra for quantum yield determination were recorded with nm bandwidth. Solutions were prepared to absorb less than 0.15 A.U. so as to prevent re-absorption and self-quenching. Then quantum yields were determined by using equation $\phi_S = \phi_r(A_r/A_s)(F_s/F_r)(n_s^2/n_r^2)$ where s and r denote the sample and reference which is ZnTPP in THF ($\phi = 0.033$)[1], respectively. A is the absorption at the excitation wavelength, F is the integrated fluorescence intensity, and n is the refractive index of the solvent.

1.3 Determination of the octanol-water partition coefficients (log $P_{o/w}$)

Octanol-water partition coefficients were calculated according to the literature.[2] Equal amounts of octanol and PBS were thoroughly mixed by an oscillator for 24 h. Each porphyrinoid was dissolved in an octanol-water system and allowed to equilibrate. Both fractions were analyzed by UV-*vis* spectra. The log $P_{o/w}$ values were calculated by the following equation:

$$\log P = \log \frac{C_{octanol}}{C_{water}}$$

$C_{octanol}$ is the molar concentration of the organic compound in the octanol phase and C_{water} is the molar concentration of the organic compound in water when the system is at equilibrium.

1.4 Determination of the *p*Ka

The titration was carried out in DMSO at ambient temperature by absorption and monitored according to the literature method.[3, 4] Triethylamine was selected as the base for measure the acid constant of **2**, because its weak nucleophilicity precluded the

possibility of nuclear attack at the lactone position.[4] However, the basicity of triethylamine is insufficient for deprotonation of **1**. Thus, pyrrolidine, which is a much stronger base than triethylamine in DMSO, was employed as the base for the titration of **1**. The working concentrations of **1** and **2** are all 5 μM. The triethylamine concentration ranges from 0.001 $mol \cdot L^{-1}$ to 0.015 $mol \cdot L^{-1}$. The pyrrolidine concentration ranged from 0.41 $mol \cdot L^{-1}$ to 1.42 $mol \cdot L^{-1}$. The *p*Ka values were calculated by the following equation:

$$H_2Por + B = HPor^- + HB^+$$

$$lgK = lg\frac{[Por^-]}{[H_2Por]} - lg[B] + lg[HB^+]$$

$$pKa(H_2Por) = -lg\,K + pKa[HB^+]$$

H_2Por or Por represent porphyrinoids and B or HB represent the base.

1.5 Determination of singlet oxygen quantum yield

Singlet oxygen quantum yields were calculated according to the literature.[5, 6] The absorbance of DPBF was adjusted to around 1.0 at 410 nm in toluene. Then, the photosensitizer was added to cuvette and photosensitizer's absorbance was adjusted to around 0.2. The solution was exposed to the halogen lamp (3 $mW \cdot cm^{-2}$) for 20s as an irradiation cycle and the absorbance was measured after each cycle. This procedure was repeated 19 times. The slope of absorbance maxima of DPBF at 410 nm versus time graph for each photosensitizer was calculated. Singlet oxygen quantum yields were determined by using Equation $\phi_{\Delta s} = \phi_{\Delta r} \cdot m_s/m_r$ where s and r denote the sample and reference which is ZnTPP in toluene ($\phi_{\Delta} = 0.68$)[1], respectively and m is the slope of the absorbance of DPBF at 410 nm versus time.

1.6 LDL Titration

Titrations of dyes in PBS (50 mM, pH = 7.4) with LDL were performed and monitored by absorption and fluorescence. The fluorescence data were analyzed according to the literature method.[7, 8] 7 μM photosensitizer was added to cuvette in PBS (50 mM, pH = 7.4), titrated with increasing concentrations of LDL and got the emission spectra by Edinburgh Instrument FLS920 Fluorescence Lifetime and Steady state spectrophotometer (ex = 415nm).

1.7 Cell Culture

Hela cells were cultured in Dulbecco's modified Eagle medium (DMEM, Gibco) supplemented with 10% fetal bovine serum (FBS), 1% penicillin and streptomycin. Hela cells were grown at 37 ℃ in a humidified atmosphere containing 5% CO_2.

1.8 Celluar uptake

Hela cells were placed on sterile glass coverslips in cell culture dishes containing complete media and allowed to grow to about 80% confluence. Complexes (1 mM dissolved in DMSO) were added to complete media to a final concentration of 2 μM. After incubated for 24 h, confocal fluorescent microscopy of living cells was performed using an FV500 scanning laser microscope (Olympus). Before imaging, cells were washed with KRBB (129 mM NaCl, 4.7 mM KCl, 1.2 mM KH_2PO4, 5 mM $NaHCO_3$, 10 mM Hepes, 3 mM Glucose, 2.5 mM $CaCl_2 \cdot 2H_2O$, 1.2 mM $MgCl_2 \cdot 6H_2O$, 0.1% BSA) 3-5 times. The slips were overlaid with KRBB and examined under confocal microscopy. The settings for confocal microscopy were as follow: 60× immersion oil

objective with resolution 512 × 512, 405 nm excitation wavelength and > 630 nm detector slit, 20% laser power, 877 PMT, 2.5 × gain, 5% offset, and 120 C.A. for our complexes. Differential interference contrast (DIC) and fluorescent images were processed and analyzed using Olympus FluoView Viewer or Image J.

1.9 Colocalization

Cells were placed on sterile glass coverslips in cell culture dishes containing complete media and allowed to grow to about 80% confluence. Complexes (1 mM dissolved in DMSO) were added to complete media to a final concentration of 2 μM. After 24 hours, cells were incubated with 1 μM LysoSensor^{TM}Yellow/Blue DND-160 for 5 min and prepared for confocal microscopy. Before imaging, cells were incubated with either 1 μM LysoSensor^{TM}Yellow/Blue DND-160 for 5 min, 1 μM ER-Tracker Green for 30 min, or 100 nM Mito Tracker Green FM for 30 min. Hela cells transfected with EGFP plasmids (EGFP-EHD1 and EGFP-FYVE, using Lipfectamine^{TM} 2000 according to manufacturer's instruction) were plated, treated with dyes as described above, and then treated for confocal imaging with the same settings for cellular uptake.

1.10 Flow Cytometry

Hela cells were grown to about 80% confluence (about 1×10^6 per well in 6-well plates) and incubated with 2 μM dyes in complete media. After 24 h, cells were then trypsinized, washed three times with PBS, resuspended in 1mL PBS and immediately analyzed on FACS Aria Ⅱ (BD Bioscience). The 405 nm laser line was used for excitation and the fluorescence signal was collected between 650 and 670 nm. 10,000 events were counted for each sample. Each group had three samples.

1.11 Cellular Uptake Mechanism of 2-Glu

The inhibition of LDL-mediated uptake of **2**-Glu into cells was performed by using heparin as an inhibitor.[9-11] Cells were incubated in serum-free media for 18 hours prior to the addition of 2 μM **2**-Glu in the presence of 100 μg·mL^{-1} LDL in serum-free media with 5 mg·mL^{-1} heparin for 5h. Then live cell images acquired or flow cytometry results were analyzed as described above. The inhibition and activation of intracellular uptake of **2**-Glu in serum-free media was performed by using D-glucose as an inhibitor and insulin as an activator. Cells were incubated in serum-free media for 18 hours and treated with 2 μM **2**-Glu in the presence of 50 mM D-glucose in serum-free media, or treated with 1μM insulin for 30 min and then incubated with 2 μM **2**-Glu in serum-free media. Then live cell images acquired or flow cytometry results were analyzed as described above.

1.12 Light-Induced Cytotoxicity Assay

The photocytotoxity assays were conducted according to the literature.[12, 13] Hela cells were seeded in flat-bottomed 96-well plates, 10^4 cells per well, with 200 μL complete culture media in the dark for 24h. After washed with PBS for three times (200 μL*3), the cells were incubated with varying concentrations from 0 μM to 12 μM **2**-Glu for another 24h in the dark while wells containing no cells are set as the controls. The cells were washed with PBS for three times and irradiated for 30 min in 100 μl PBS with visible light (400-700 nm, 6.5 mW·cm^{-2}). Then PBS was replaced by 200 μL fresh culture media. After cultured for 24 h, the cells were washed with PBS three times (200 μL*3). 10 μL Cell Counting Kit-8 (CCK-8) solution and 90 μl PBS were added per well. After 2 hours, the absorbance at 450nm was read by 96-well plates reader. The viability of Hela cells was calculated by the following equation:

$$CV=（As-Ab）/（Ac-Ab）\times 100\%$$

CV stands for the viability of cells，As, Ac and Ab stand for the absorbance of cells containing **2**-Glu, cell control(0 μM **2**-Glu) and blank control (wells containing neither cells nor **2**-Glu).

1.13 Determination of Intracellular ROS level

Intracellular ROS detection was operated according to the literature.[14, 15] ROS detection reagent (H2DCFDA) was purchased from Invitrogen (LifeTechnologies) and images of living cells were performed using Nikon A1R-si Laser Scanning Confocal Microscope (Japan), equipped with lasers of 405/488/543/638 nm.

Hela cells were placed on poly-D-lysine-coated sterile glass coverslips in cell culture dishes containing complete media 2 ml for 24 h. Then **2**-Glu (1 mM dissolved in DMSO) was added to complete culture media with different final concentrations for another 24 h. After washed with PBS for three times, culture media with 10 mM H2DCFDA was added to the dishes and the cells was incubated for 30 min. After washed three times with PBS, they were immerged in 1ml PBS and irradiated for 30 min with visible light (400-700 nm, 6.5 $mW \cdot cm^{-2}$). Cells were imaged via the fluorescence mode with a 60× immersion lens with the following parameters: laser power 100%, pinhole 4.0 A.U., excitation wavelength 405 and 488 nm, detector slit 552-617 nm, resolution 1024×1024, and a scan speed 0.5 frame per second. Intracellular ROS intensities were calculated by ImageJ with more than 30 cells.

For the light dose effect on ROS, Hela cells were placed on poly-D-lysine-coated sterile glass coverslips in cell culture dishes containing complete media 2 ml for 24 h. Then **2**-Glu (1 mM dissolved in DMSO) was added to complete culture media with a final concentration of 8 μM for another 24 h. After washed with PBS for three times, culture media with 10 mM H2DCFDA was added to the dishes and the cells were incubated for 30 min. After washed three times with PBS, they were immerged in 1 ml PBS and irradiated for different times with visible light (400-700 nm) of 6.5 $mW \cdot cm^{-2}$. Before confocal imaging, cells were stained with Hoechst 33342 for 10 min. Cells were imaged via the fluorescence mode with a 60× immersion lens with the following parameters: laser power 100%, pinhole 4.0 A.U., excitation wavelength 405 and 488 nm, detector slit 552-617 nm, resolution 1024×1024, and a scan speed 0.5 frame per second. The control experiment was conducted without **2**-Glu under the same conditions. Intracellular ROS intensities were calculated by ImageJ with more than 30 cells.

2. Synthesis and Characterization:

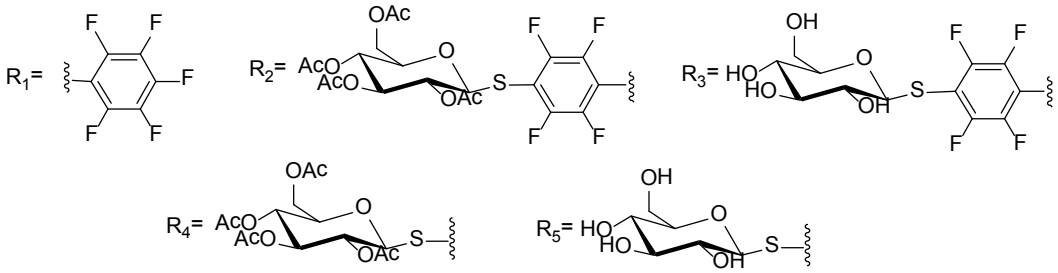

Scheme S1 List of symbols for functional groups

In order to make the article more concise, the Rs will represent the corresponding functional groups in the following contents.

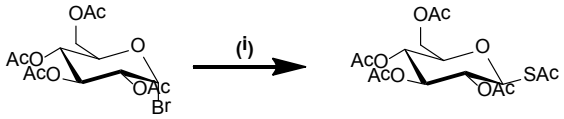

Glu$_{(OAc)_4}$-Br **Glu$_{(OAc)_4}$-SAc**

Scheme S2 Synthetic route for Glu(OAc)$_4$-SAc: (i) 2 eq. potassium ethanethioate, dry acetone, r.t., overnight.

Glu(OAc)$_4$-SAc: 2,3,4,6-tetra-O-acetyl-glucosyl thioacetate

Glu(OAc)$_4$-SAc was prepared by the literature method (isolated yield: 78%).[161] ^{1}H NMR ($CDCl_3$, 300 MHz): δ 2.01, 2.02, 2.03, 2.08 (4S, 12H), 2.39 (s, 3H, $SCOCH_3$), 3.84 (m, 1H), 4.10 (dd, 1H, J = 10.5 Hz, J = 2.1 Hz), 4.26 (dd, 1H, J = 7.5 Hz, J = 5.4 Hz), 5.13 (m, 2H), 5.28 (t, 2H, J = 8.1 Hz). ESI-MS: $[M+Na]^+$*calc.* for $[C_6H_{22}NaO_{10}S]^+$, 429.1, found: 429.1.

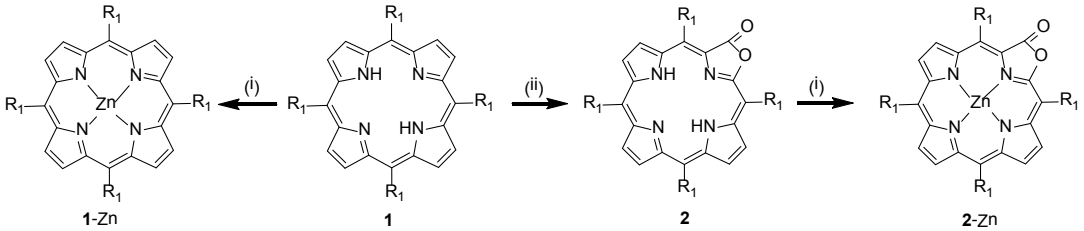

1-Zn **1** **2** **2**-Zn

Scheme S3 Synthetic route for **2**, **1**-Zn, **2**-Zn**:** (i) 10 eq. $Zn(OAc)_2$, $CHCl_3$: MeOH = 1:1, N_2, reflux, 3 h (ii) 24 eq. $AgNO_3$, HOAc, N_2, reflux, 12 h.

H_2F_{20}TPP (1): 5,10,15,20-Tetrakis (2,3,4,5,6-tetrafluorophenyl) porphyrin

H_2F_{16}TPPL, ZnF_{20}TPPL and ZnF_{20}TPP were prepared according to the literature.[17]

H_2F_{20}TPPL (2):5,10,15,20-tetrakis(2,3,4,5,6-pentafluorophenyl) porpholactone

A mixture of 1 eq. F_{20}TPP (20.0 mg, 0.02 mmol), 24eq. AgOTf (126.0 mg, 0.48 mmol), and 5eq. NaOAc (8.2 mg, 0.10 mmol), were dissolved in 2 mL acetic acid, the solution was stirred and refluxed under nitrogen for 12 h. The purple solution was evaporated under reduced pressure, then purified by column chromatography (petroleumether: methylene chloride = 4:1), the product was purple solid (Yield: 30%). ^{1}H NMR (d^6-dmso, 300 MHz): δ9.77–9.18 (m, 4H), 9.03 (dd, J = 24.4, 4.8 Hz, 2H), -1.99 (s, 1H), -2.29 (s, 1H).^{19}FNMR (d^6-dmso, 282 MHz): δ 24.52 (d, 2F, J = 18.3 Hz), 23.85–23.52 (m, 4F), 23.44 (d, 2F, J = 18.6 Hz), 11.08 (t, 1F, J = 22.2 Hz), 9.98 (t, J = 22.3 Hz, 2F), 9.39 (dd, 2F, J = 52.0 and 22.8 Hz), 1.17 (t, 4F, J = 20.2 Hz), 0.61 (t, 2F, J = 23.3 Hz), 0.30 (t, 2F, J = 20.2 Hz). HRMS (ESI): $[M+Na]^+$*calc.* for $[C_{43}H_8F_{20}N_4NaO_2]^+$, 1015.0223, found: 1015.02201.

$ZnF_{20}TPPL$ (2-Zn): Zinc5,10,15,20-Tetrakis (2,3,4,5,6-tetrafluorophenyl) porpholactone

Compound **1** (100.0 mg, 100.8 μmol) and Zinc acetate ($Zn(OAc)_2 \cdot 2H_2O$, 221.9 mg, 1.01 mmol) were dissolved in 5 mL chloroform and 5 mL methanol. The solution was refluxed for 3 h and then evaporated under reduced pressure. The deep blue solid product (96.7 mg, yield: 91%) was purified by column chromatography (hexane: methylene chloride = 1:1). ^{1}H NMR ($CDCl_3$, 400 MHz): δ 8.79 (d, J = 4.8 Hz, 1H), 8.76-8.71 (m, 3H), 8.66 (dd, J = 8.0, 4.7 Hz, 1H). MS (ESI): $[M+H]^+$*calc.* for $[C_{43}H_7F_{20}N_4O_2Zn]^+$, 1054.9, found: 1055.0, $[M+Na]^+$*calc.* for $[C_{43}H_6F_{20}N_4NaO_2Zn]^+$, 1076.9, found: 1076.9.

$ZnF_{20}TPP$ (1-Zn): Zinc5,10,15,20-Tetrakis (2,3,4,5,6-tetrafluorophenyl) porphyrin

Compound **2** (100.0 mg, 102.5 μmol) and Zinc acetate ($Zn(OAc)_2 \cdot 2H_2O$, 225.7 mg, 1.03 mmol) were dissolved in 5 mL chloroform and 5 mL methanol. The solution was refluxed for 3 h and then evaporated under reduced pressure. The red solid product (97.6 mg, yield: 92%) was purified by column chromatography (hexane: methylene chloride = 1:1). ^{1}H NMR ($CDCl_3$, 400 MHz): δ 9.01 (s, 8H). MS (ESI): $[M+H]^+$*calc.* for $[C_{44}H_9F_{20}N_4Zn]^+$, 1036.9, found: 1037.0.

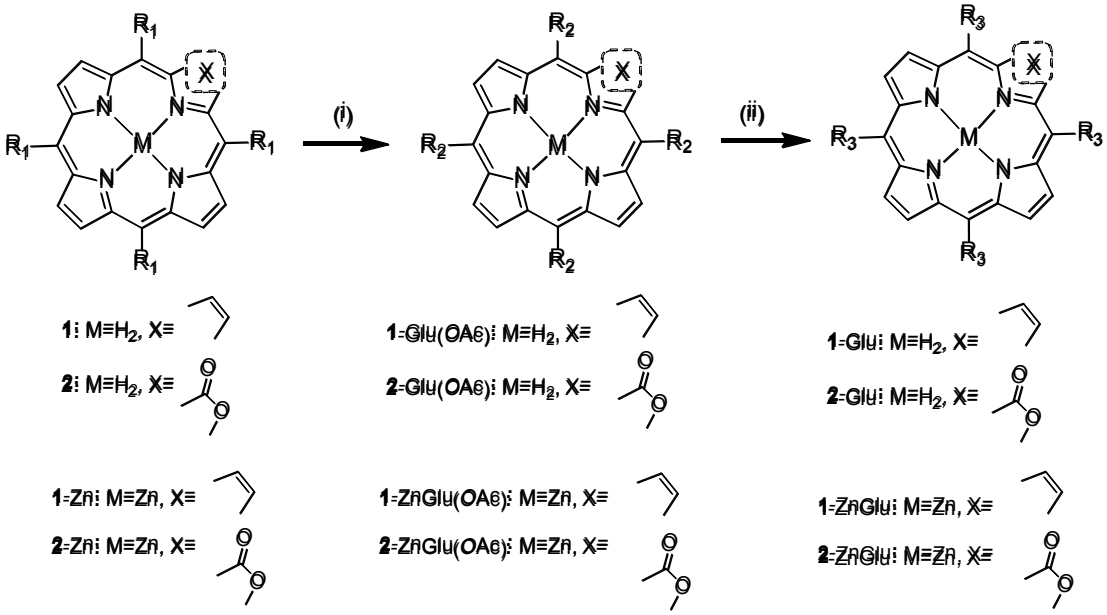

Scheme S4 Synthetic route for **1**-Glu**, 2**-Glu**, 1**-ZnGlu**, 2**-ZnGlu**:** (i) 8 eq. $Glu(OAc)_4$-SAc,Diethylamine, DMF, N_2, r.t., 8 h (ii) 16 eq. $NaOCH_3$, DCM: MeOH = 1:1, N_2, r.t., 1 h.

H_2F_{16}TPP-S-Glu(*O*Ac)$_4$ (1-Glu(*O*Ac))**:** 5,10,15,20-tetrakis(4-1'-thio-2',3',4',6'-tetraacetylglucosyl-2,3,5,6-tetrafluorophenyl) porphyrin

H_2F_{16}TPP-S-Glu(*O*Ac)$_4$ was prepared according to the procedure described in the literature.[16] Compound **2** (20.0 mg, 20.5 μmol) and Glu(*O*Ac)$_4$-SAc (66.7 mg, 164 μmol) were dissolved in 5 mL DMF and 0.5 mL diethyl amine, the solution was stirred for 8 h at room temperature. Evaporated the purple solvent under reduced pressure and purified the purple solid product (20.5 mg, yield: 43%) by column chromatography, petroleumether: ethyl acetate (1:2) as eluent. ^{1}H NMR ($CDCl_3$, 400 M Hz): δ -2.85 (s, 2H), 2.09-2.11(m, 36H), 2.24 (s, 12H), 3.91 (m, 4H), 4.32 (d, 8H, *J* = 3.2 Hz), 5.18 (d, 4H, *J* = 10.0 Hz), 5.25 (m, 8H), 5.38 (t, 4H, *J* = 9.2 Hz), 9.04 (s, 8H). ^{19}F NMR ($CDCl_3$, 282 MHz) δ16.02 (m, 8F), 12.16-11.39 (m, 8F). MS(MALDI-TOF): $[M+Na]^+$*calc.* for $[C_{99}H_{84}F_{16}N_4NaO_{38}S_4]^+$, 2391.32831, found: 2391.33319. MS (MALDI-TOF**),** $[M+H]^+$*calc.* for $[C_{100}H_{87}F_{16}N_4O_{36}S_4]^+$, 2352.4, found: 2352.1.

H_2F_{16}TPPL-S-Glu(*O*Ac)$_4$ (2-Glu(*O*Ac))**:**

5,10,15,20-tetrakis(4-1'-thio-2',3',4',6'-tetraacetylglucosyl-2,3,5,6tetrafluorophenyl)-porpholactone

H_2F_{16}TPPL-S-Glu(*O*Ac)$_4$ was prepared according to the procedure described in the literature.[16] Compound **1** (18.0 mg, 18.1 μmol) and Glu(*O*Ac)$_4$-SAc (58.9 mg, 145.0 μmol) were dissolved in 5mL DMF and 0.5 mL diethyl amine, the solution was stirred for 8hat room temperature. Evaporated the purple solution under reduced pressure and purified the purple solid product (17.6 mg, yield: 41%) by column chromatography, hexane: ethyl acetate (2:3) as eluent. ^{1}H NMR ($CDCl_3$, 400 M Hz): -2.06 (s, 1H), -1.76 (s, 1H), 2.09 (m, 36H), 2.22 (s, 12H), 3.91 (m, 4H), 4.31 (m, 8H) 5.23 (m, 12H), 5.37 (t, 4H, *J* = 9.2 Hz), 8.71(dd, 2H, *J* = 26.4 Hz, *J* = 4.8 Hz), 8.98 (m, 4H). ^{19}F NMR ($CDCl_3$, 282 MHz): δ 27.45-26.57 (m, 5F), 26.59-26.07 (m, 1F), 25.74 (m, 1F), 21.97–21.60 (m, 4F), 21.58-21.27 (m, 2F), 20.06 (m, 2F). HRMS (ESI): $[M+Na]^+$*calc.* for $[C_{99}H_{84}F_{16}N_4NaO_{38}S_4]^+$, 2391.32831, found: 2391.33319.

ZnF_{16}TPP-S-Glu(*O*Ac)$_4$ (1-ZnGlu(*O*Ac))**:**

Zinc5,10,15,20-Tetrakis(4-1'-thio-2',3',4',6'-tetraacetylglucosyl-2,3,5,6-tetrafluorophenyl) porphyrin

ZnF_{16}TPPL-S-Glu(*O*Ac)$_4$ was prepared according to the procedure described in the literature.[16] ZnF_{20}TPP (20.0 mg, 19.3 μmol) and Glu(*O*Ac)$_4$-SAc (63.0mg, 155.0 μmol) were dissolved in 5mL DMF and 0.5 mL diethyl amine, the solution was stirred for 8 h at room temperature. Evaporated the red solution under reduced pressure and purified the red solid product by column chromatography (hexane: ethyl acetate = 1:2). ^{1}H NMR ($CDCl_3$, 400 M Hz): 8.95 (s, 8H), 5.18-5.12 (m, 4H), 5.08-5.00 (m, 12H), 4.08 (d, J = 3.5 Hz, 8H), 3.77-3.72 (m, 12H), 2.05 (s, 12H), 1.88 (s, 36H).

ZnF_{16}TPPL-S-Glu(*O*Ac)$_4$ (2-ZnGlu(*O*Ac))**:**

Zinc5,10,15,20-tetrakis(4-1'-thio-2',3',4',6'-tetraacetylglucosyl-2,3,5,6-tetrafluorophenyl)-porpholactone

ZnF_{16}TPPL-S-Glu(*O*Ac)$_4$ was prepared according to the procedure described in the literature. [16]ZnF_{20}TPPL (20.0 mg, 19.0 μmol) and Glu(*O*Ac)$_4$-SAc (61.8 mg, 152.0 μmol) were dissolved in 5mL DMF and 0.5 mL diethyl amine, the solution was stirred for 8 h at room temperature. Evaporated the deep blue solution under reduced pressure and purified the deep blue solid product by column chromatography (hexane: ethyl acetate = 1:2). ^{1}H NMR ($CDCl_3$, 400 M Hz): 8.79 (d, J = 4.6 Hz, 1H), 8.72

(dd, J = 11.7 Hz, 6.1 Hz, 3H), 8.64 (d, J = 4.1 Hz, 2H), 5.20-4.91 (m, 16H), 4.01 (m, 8H), 3.76-3.64 (m, 4H), 2.00 (m, 12H), 1.91-1.81 (m, 36H).

H_2F_{16}TPPL-S-GluOH$_4$ (2-Glu**):** 5,10,15,20-Tetrakis (4-1'-thio-glucosyl-2,3,5,6-tetrafluorophenyl) porpholactone

H_2F_{16}TPPL-S-GluOH$_4$ was prepared according to the procedure described in the literature.[16] **2**-Glu(*O*Ac)was treated with 16 equiv $NaOCH_3$ at room temperature in the mixed solution of methanol: methylene chloride (v: v = 1:1) and the reaction was monitored by TLC. The purple solid product (Yield: 80%) was purified by column chromatography. ^{1}H NMR (CD_3OD, 300 M Hz): 9.24-9.05 (m, 4H), 8.80 (*J* = 2.1 Hz, *J* = 28.2 Hz), 5.15 (m, 4H), 3.97 (m, 4H), 3.75 (m, 4H), 3.52-3.42 (m, 16H). ^{19}FNMR (CD_3OD, 282 MHz): δ 28.00-27.42 (m, 6F), 27.10 (m, 2F), 21.90 (m, 2F), 21.53 (m, 4F), 20.60 (m, 2F). HRMS (ESI): $[M+Na]^+$*calc.* for $[C_{67}H_{52}F_{16}N_4NaO_{22}S_4]^+$, 1719.15927, found: 1719.15684.

H_2F_{16}TPP-S-GluOH$_4$ (1-Glu**):** 5,10,15,20-Tetrakis(4-1'-thio-glucosyl-2,3,5,6-tetrafluorophenyl)porphyrin

H_2F_{16}TPPL-S-GluOH$_4$ was prepared according to the procedure described in the literature.[16] **1**-Glu(*O*Ac) was treated with 16 equiv $NaOCH_3$ at room temperature in the mixed solution of methanol: methylene chloride (v: v = 1: 1) and the reaction was monitored by TLC. The purple solid product (Yield: 90%) was purified by column chromatography. ^{1}H NMR (CD_3OD, 300 M Hz): 8.99 (s, 8H), 5.09 (m, 4H), 3.91 (m, 4H), 3.68 (m, 4H), 3.43-3.20 (m, 16H). ^{19}F NMR(CD_3OD, 282 MHz) δ23.15 (dd, *J* = 24.6, 11.7 Hz, 8F), 17.75 (dd, *J* = 24.6, 11.7 Hz, 8F). HRMS (ESI): $[M+Na]^+$*calc.* for $[C_{68}H_{54}F_{16}N_4NaO_{20}S_4]^+$, 1701.18432, found: 1701.18510.

ZnF_{16}TPP-S-GluOH$_4$ (1-ZnGlu**):** Zinc5,10,15,20-Tetrakis (4-1'-thio-glucosyl-2,3,5,6-tetrafluorophenyl) porphyrin

ZnF_{16}TPP-S-GluOH$_4$ was prepared according to the procedure described in the literature.[16] **1**-ZnGlu(*O*Ac)was treated with 16 equiv $NaOCH_3$ at room temperature in the mixed solution of methanol: methylene chloride (v: v =1: 1) and the reaction was monitored by TLC. The red solid was purified by column chromatography (15.5 mg, yield: 46%). ^{1}H NMR (CD_3OD, 400 M Hz): δ9.10 (s, 8H), 5.20 (m, 4H), 4.04 (m, 4H), 3.78 (m, 4H), 3.57-3.45 (m, 16H). ^{19}F NMR (CD_3OD, 282 MHz): δ 21.89 (m, 8F), 17.48 (m, 8F). MS (MALDI): $[M]^+$*calc.* for $[C_{68}H_{52}F_{16}N_4O_{20}S_4Zn]^+$, 1742.1089, found: 1742.1493.

ZnF_{16}TPPL-S-GluOH$_4$ (2-ZnGlu**):** Zinc5,10,15,20-Tetrakis (4-1'-thio-glucosyl-2,3,5,6-tetrafluorophenyl) porpholactone

ZnF_{16}TPPL-S-GluOH$_4$ was prepared according to the procedure described in the literature.[16] **2**-ZnGlu(*O*Ac)was treated with 16 equiv $NaOCH_3$ at room temperature in the mixed solution of methanol: methylene chloride (v: v = 1: 1) and the reaction was monitored by TLC. The purple solid was purified by column chromatography(15.2 mg, yield: 45%).^{1}H NMR (CD_3OD, 400 M Hz): δ8.94 (m, 1H), 8.92-8.83 (m, 3H), 8.82-8.75 (m, 2H), 5.13 (m, 4H), 3.96 (m, 4H), 3.76 (m, 4H), 3.53-3.40 (m, 16H). ^{19}F NMR (CD_3OD, 282 MHz): δ 22.23 (m, 6F), 21.67 (m, 2F), 16.98 (m, 6F), 16.04 (m, 2F). MS (MALDI): $[M+Na]^+$*calc.* for $[C_{67}H_{50}F_{16}N_4NaO_{22}S_4Zn]^+$, 1783.0729, found: 1783.0043.

3. Supporting Tables

Table S1 Photophysical data for porphyrinoids studied in this work.

Compound	λ_{Soret} /nm (logε) [c]	λ_Q /nm (logε) [c]				λ_{em} (nm)	Φ[d]
1[a]	412 (5.14)	506 (3.98)	540 (2.96)	582 (3.46)	636 (2.38)	641,707	0.04
2[a]	409 (5.18)	510 (3.95)	545 (3.81)	589 (3.60)	642 (4.03)	646, 713(shoulder)	0.13
1-Glu[b]	410 (5.02)	506 (3.86)	540 (2.71)	581 (3.31)	634 (2.04)	640,706	0.07
2-Glu[b]	410 (5.12)	506 (3.96)	540 (4.86)	586 (3.83)	641 (3.96)	644, 713(shoulder)	0.18
3-Glu[b]	417 (5.59)	515 (4.21)	552 (4.04)	592 (3.73)	648 (3.72)	652, 716	0.09
4-Glu[b]	427 (4.50)	523 (2.87)	563 (3.17)	607 (3.26)	-	639, 705(shoulder)	0.03
1-ZnGlu[b]	419 (5.51)	-	551 (4.15)	-	-	592, 644	0.02
2-ZnGlu[b]	422 (5.38)	-	562 (3.96)	607 (4.40)	-	609, 664(shoulder)	0.04

[a] Measurements were performed in dichloromethane. [b] Measurements were performed in methanol. [c] The extinction coefficient ε was in $M^{-1}cm^{-1}$. [d] Fluorescence quantum yield are based on the value of 0.033 for ZnTPP in THF at room temperature.

Table S2 LDL Binding Constants of porphyrinoids studied in this work.

Compound	**1**-Glu	**2**-Glu	**3**-Glu	**4**-Glu	**1**-ZnGlu	**2**-ZnGlu
I/I_0	6.19501	0.77323	4.7882	0.50666	0.61391	0.42716
Binding Constant (M^{-1})	-	2.45×10^{8}	6.99×10^{6}	-	-	-

Table S3 Serum-dependent Pearson's coefficient of **2**-Glu with different trackers.

Trackers	Serum free media	BSA[a]	LDL[b]	Complete media
LysoSensor™Yellow/Blue	0.77	0.77	0.85	0.79
FYVE-EGFP	0.67	0.69	0.61	0.58
EHD1-EGFP	0.67	0.65	0.59	0.50
Mito Tracker Green FM	0.47	0.55	0.50	0.56
ER-Tracker Green	0.48	0.45	0.50	0.47

[a] Serum free media with 100 μg·mL^{-1} BSA. [b] Serum free media with 100 μg·mL^{-1} LDL.

4. Supporting Figures

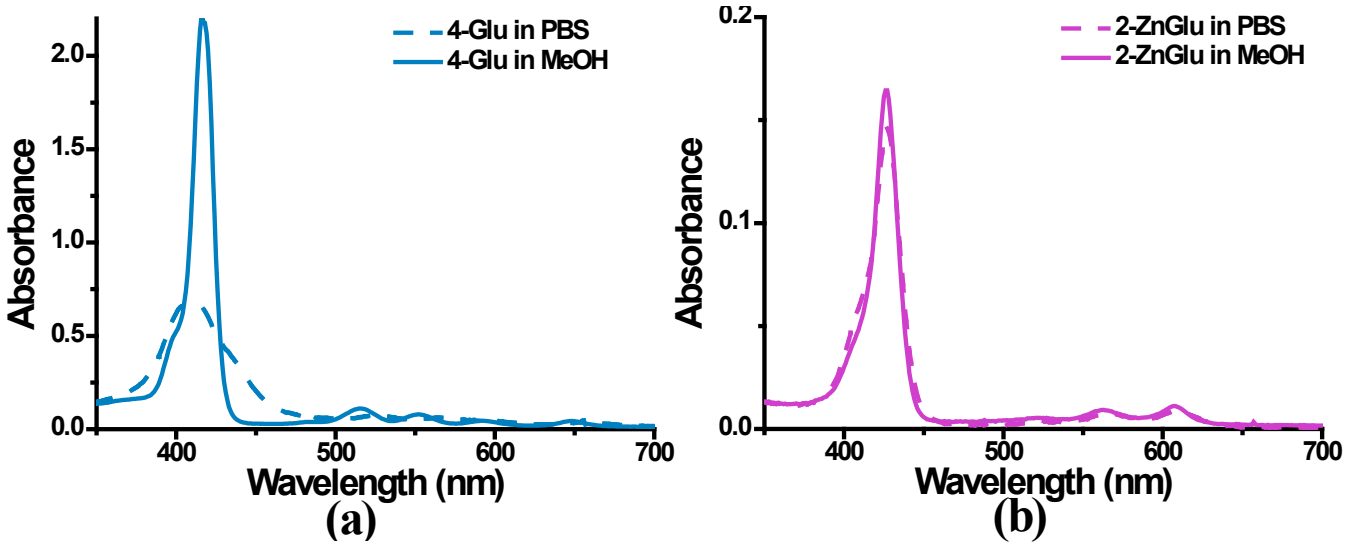

Figure S1 Absorption spectra of **4**-Glu and **2**-ZnGlu in PBS and methnol.

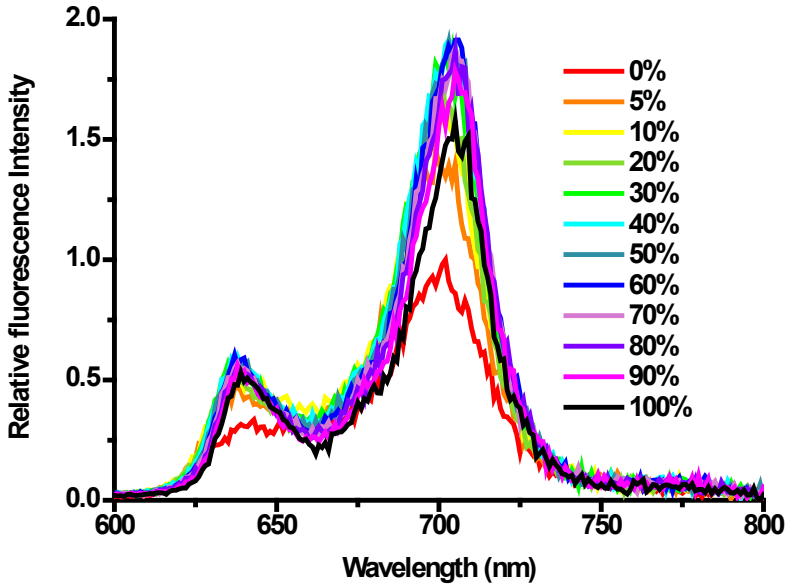

Figure S2 Emission spectra of **1**-Glu in the mixed solvent of methanol and water (v: v).

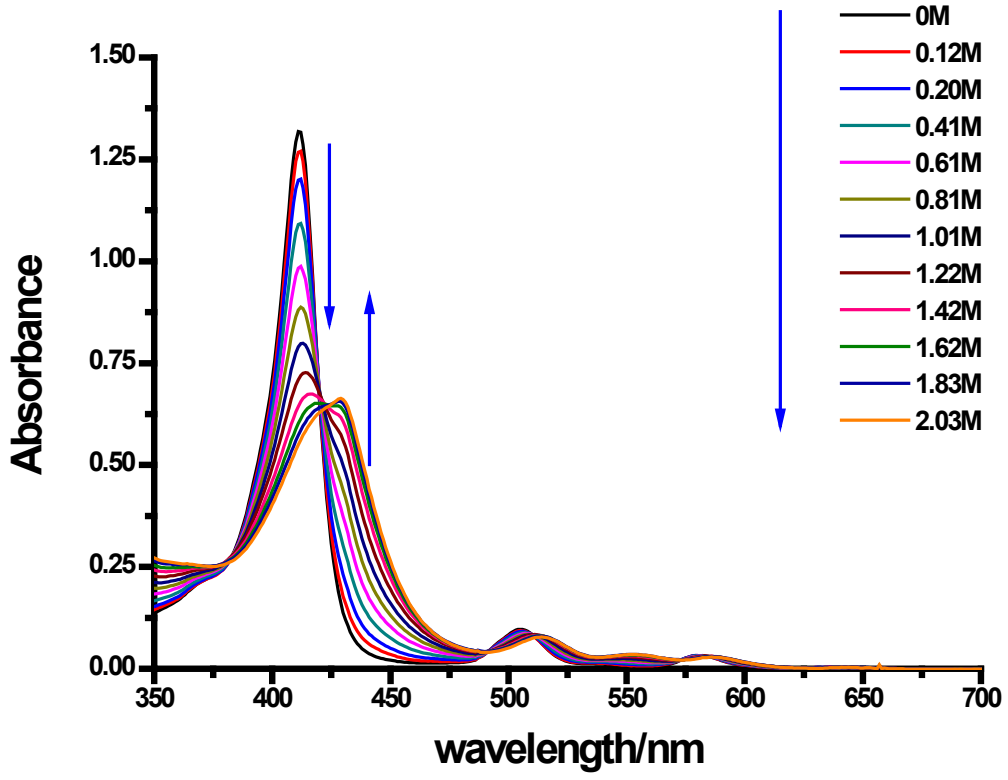

Figure S3 Absorption spectra of **1** (5 μM) treated with various amounts of pyrrolidine in DMSO.

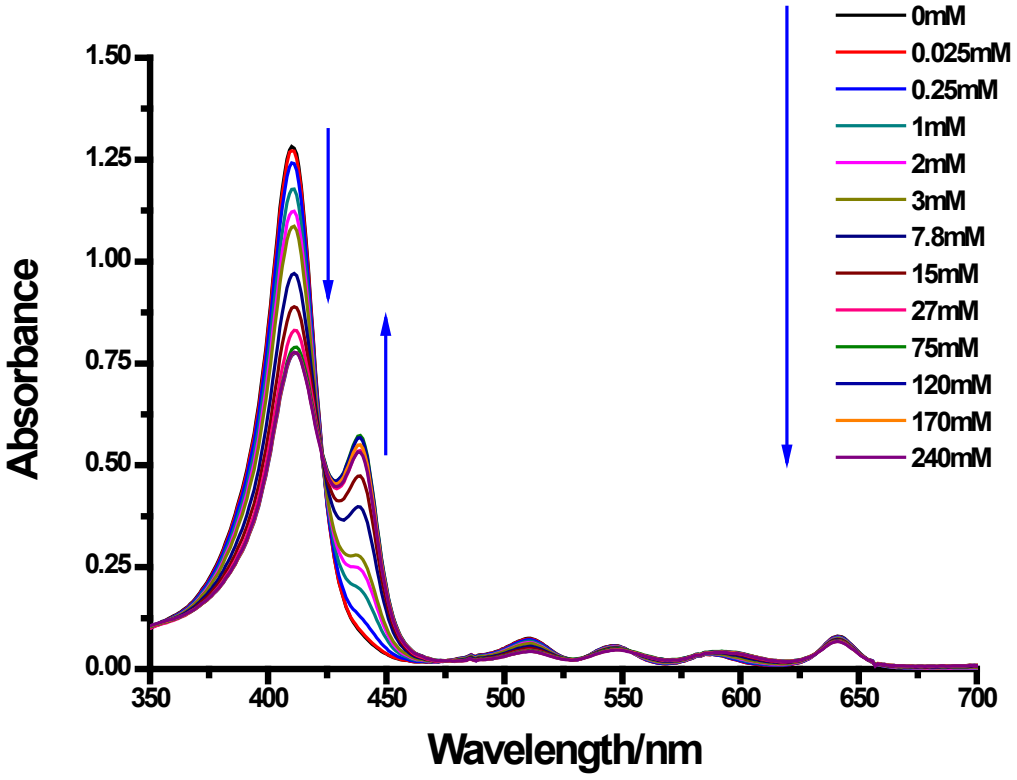

Figure S4 Absorption spectra of **2** (5 μM) treated with various amounts of triethylamine in DMSO.

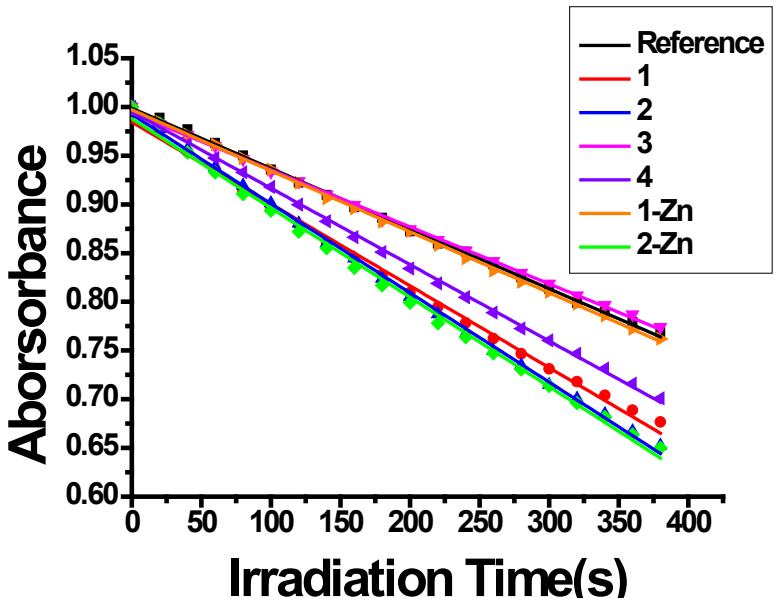

Figure S5 Singlet oxygen quantum yields of porphyrinoids: Absorbance decrease of DPBF at 410 nm versus irradiation time in the presence of porphyrinoids studied in this work. [a] ZnTPP in toluene was set as reference. [b] lightsource: visible light (400-700 nm, 3 $mW \cdot cm^{-2}$).

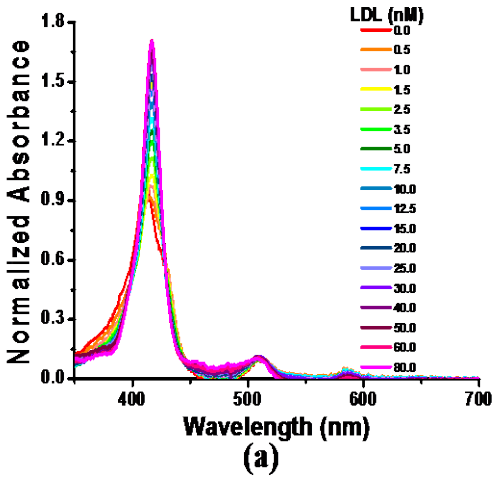

Figure S6 LDL binding experiment with **1**-Glu. (a) Absorption spectra of 7 μM **1**-Glu with increasing concentrations of LDL in PBS.

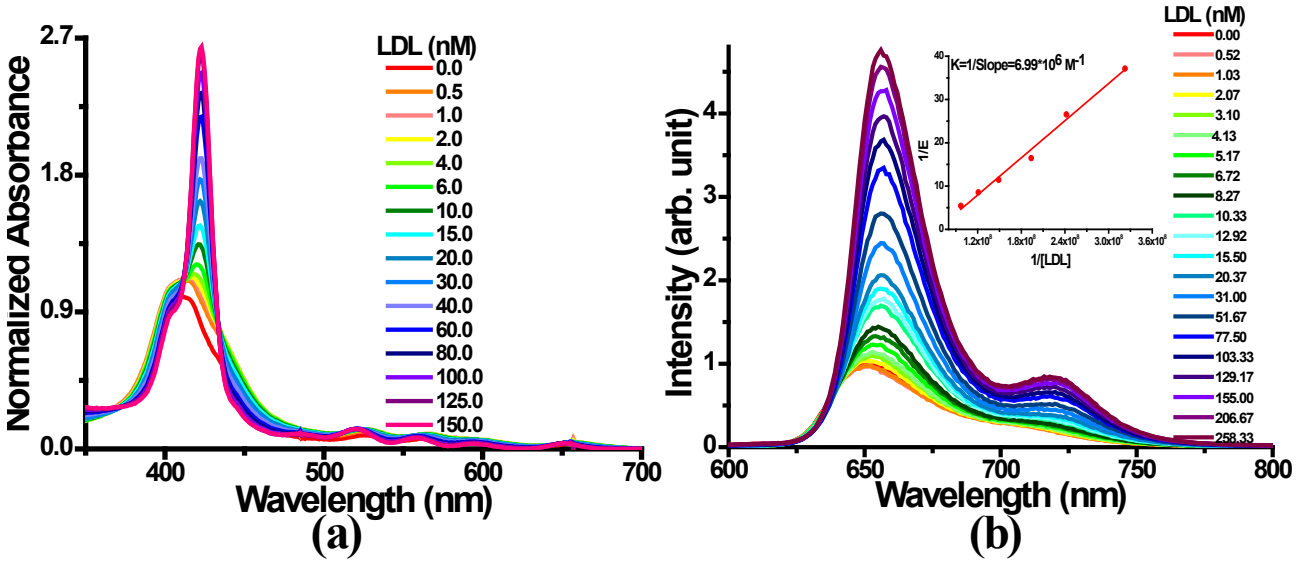

Figure S7 LDL binding experiment with **3**-Glu. (a) Absorption spectra of 7 μM **3**-Gluwith increasing concentrations of LDL in PBS. (b) Emission spectra of 7μM **3**-Glu with increasing LDL concentrations (0-258.3 nM) in PBS (ex = 417 nm) and the inset shows InversePlot ($K = 6.99 \times 10^6\ M^{-1}$).

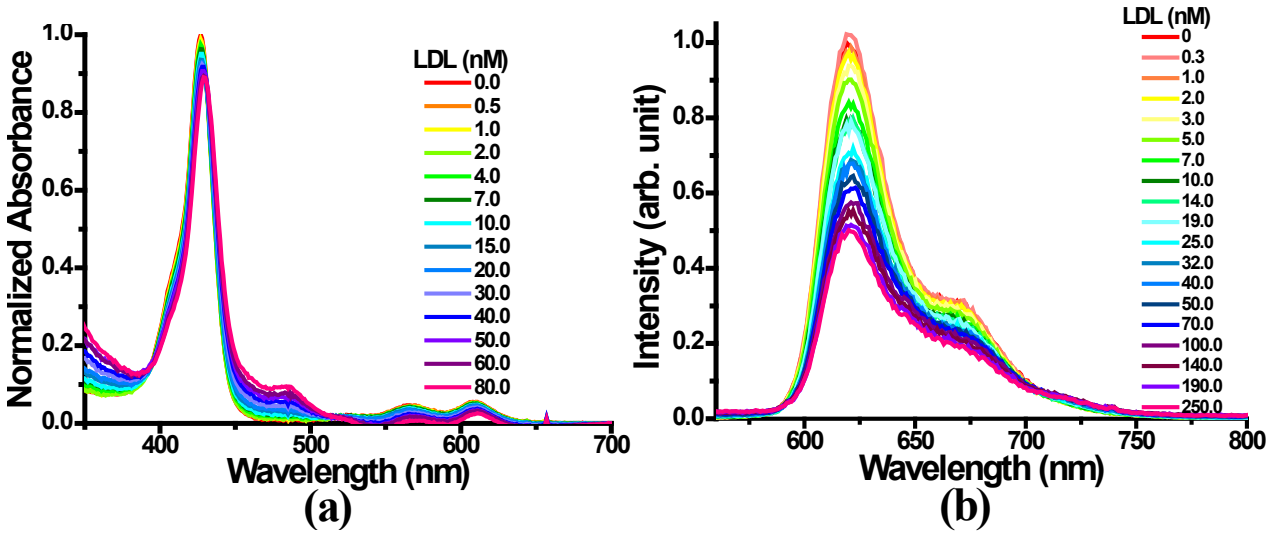

Figure S8 LDL binding experiment with **4**-Glu. (a) Absorption spectra of 7 μM **4**-Glu with increasing concentrations of LDL in PBS. (b) Emission spectra of 7 μM **4**-Glu with increasing LDL concentrations (0-250.0 nM) in PBS (ex = 428nm).

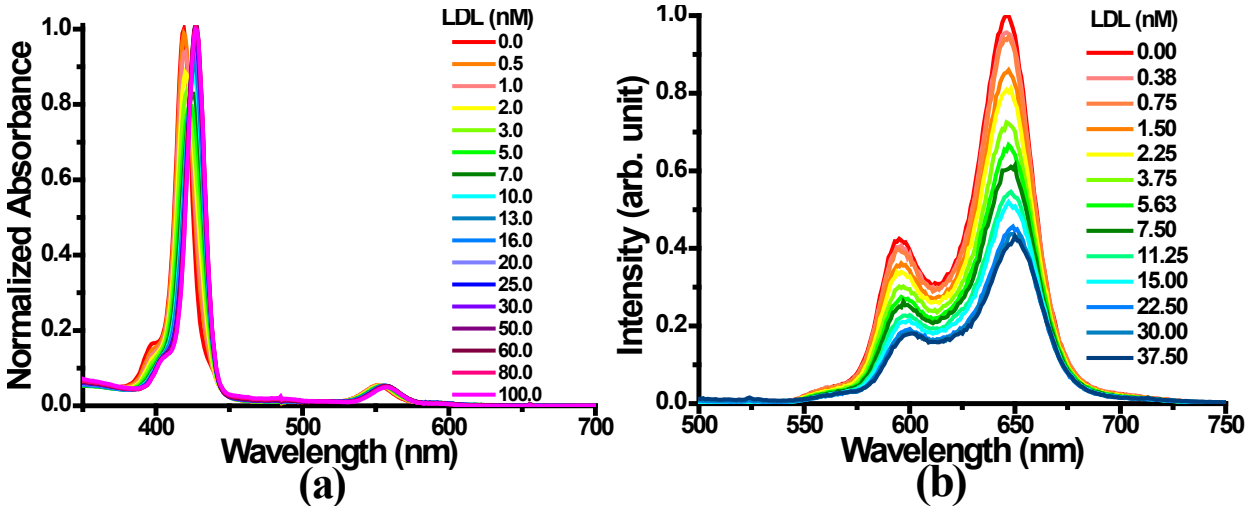

Figure S9 LDL binding experiment with **1**-ZnGlu. (a) Absorption spectra of 7 μM **1**-ZnGlu with increasing LDL concentrations in PBS. (b) Emission spectra of 7 μM **1**-ZnGlu with increasing LDL concentrations (0-37.5 nM) in PBS (ex = 413nm).

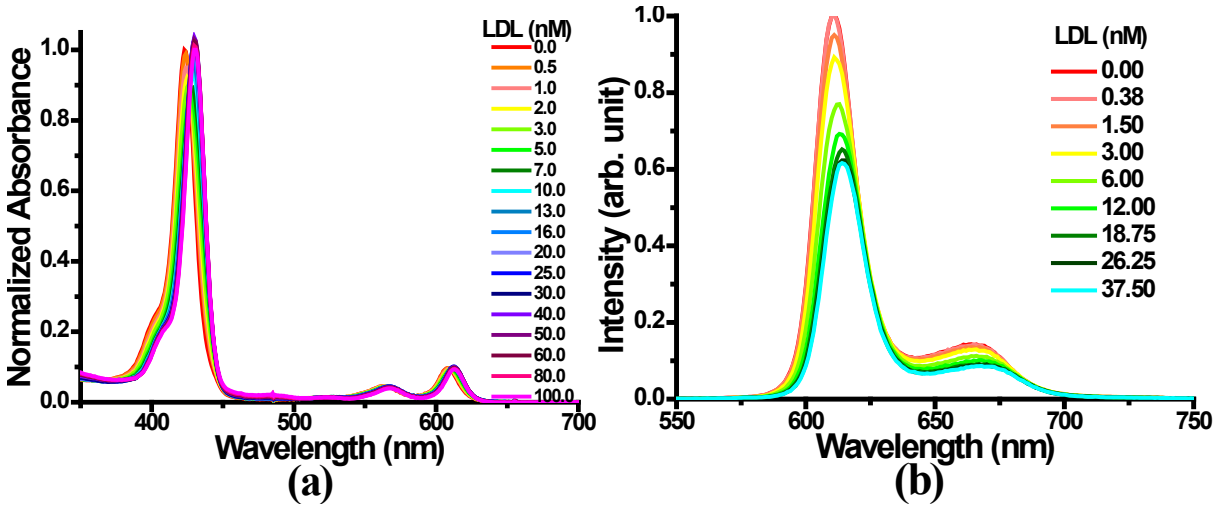

Figure S10 LDL binding experiment with **2**-ZnGlu. (a) Absorption spectra of 7 μM **2**-ZnGlu with increasing LDL concentrations in PBS. (b) Emission spectra of 7 μM **2**-ZnGlu with increasing LDL concentrations (0-37.5 nM) in PBS (ex = 418nm).

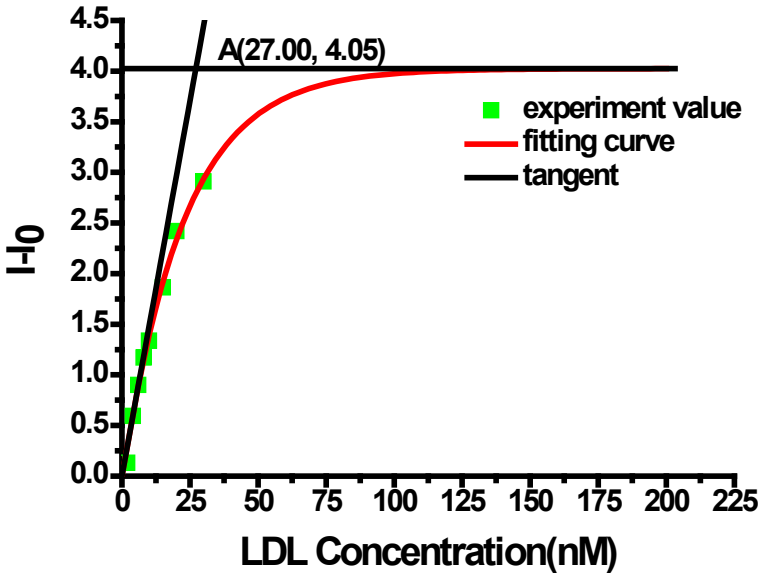

Figure S11 Binding ratio of **2**-Glu to LDL. Fluorescence changes at the maximum emission of **2**-Glu (5×10^{-6} M) titrated with increasing concentrations of LDL (ex = 415 nm). The intercept between the plateau value and the initial slope of the curve is 27.00×10^{-9} M. The maximum capacity of LDL to bind **2**-Glu is the ratio between **2**-Glu concentration and this intercept, *ca*. 185 molecules.

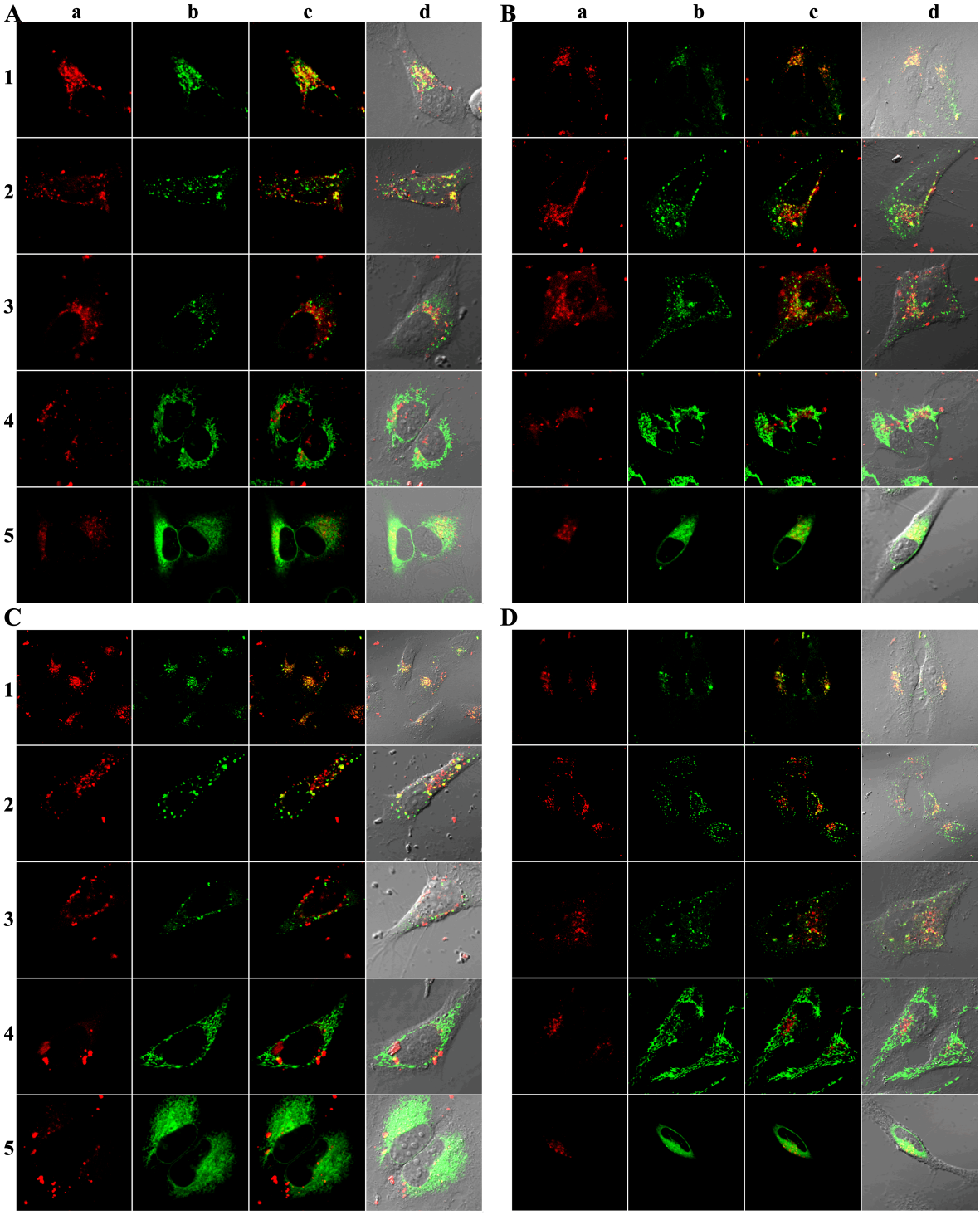

Figure S12 Serum-dependent subcellular localization of **2**-Glu. Hela cells were pre-incubated in serum-free media for 18 h and then treated with 2 μM **2**-Glu in (A) serum-free media; (B) serum-free media with 100 μg·mL^{-1} BSA; (C) serum-free media with 100 μg·mL^{-1} LDL; (D) complete media for 5 h. Column (a) image of **2**-Glu. Column (b) image of commercial markers. Column (c) merged images of (a) and (b). Column (d) merged images of (c) and DIC. Row (1) co-localization study of dye and LysoSensor^{TM}Yellow/Blue DND-160. Row (2) co-localization study of dye and early endosome marker EGFP-FYVE. Row (3) co-localization study of dye and recycling endosomes marker EGFP-EHD1. Row (4) co-localization study of dye and Mito Tracker Green FM. Row (5) co-localization study of dye and ER-Tracker Green.

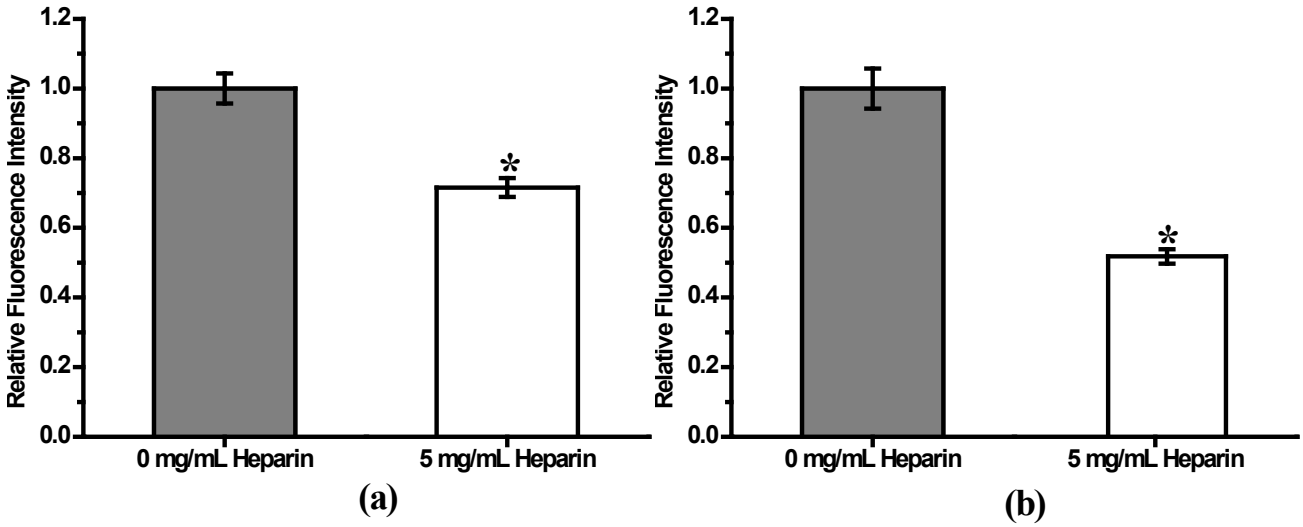

Figure S13 The effect of heparin on the cellular uptake of **2**-Glu in different media. The relative cellular fluorescence intensity in presence of 0 $mg \cdot mL^{-1}$ or 5 $mg \cdot mL^{-1}$ heparin was measured from the confocal images in (a) complete media, (b) serum-free media with 100 $\mu g \cdot mL^{-1}$ LDL. The significance of the differences between the mean values were demonstrated by $p<0.001$ and marked by *. (Mean ±SD, each condition contains 13-36 cells)

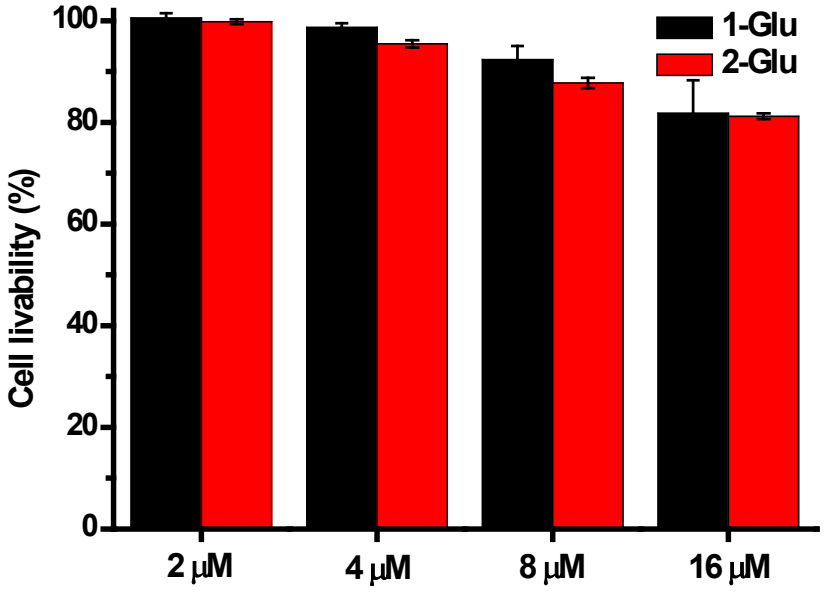

Figure S14 Dark cytotoxicity of **1**-Glu and **2**-Glu toward Hela cells using CCK-8 assay. Hela cells were incubated 2-16 μM dye for 24 h in complete media. (Mean ±SD)

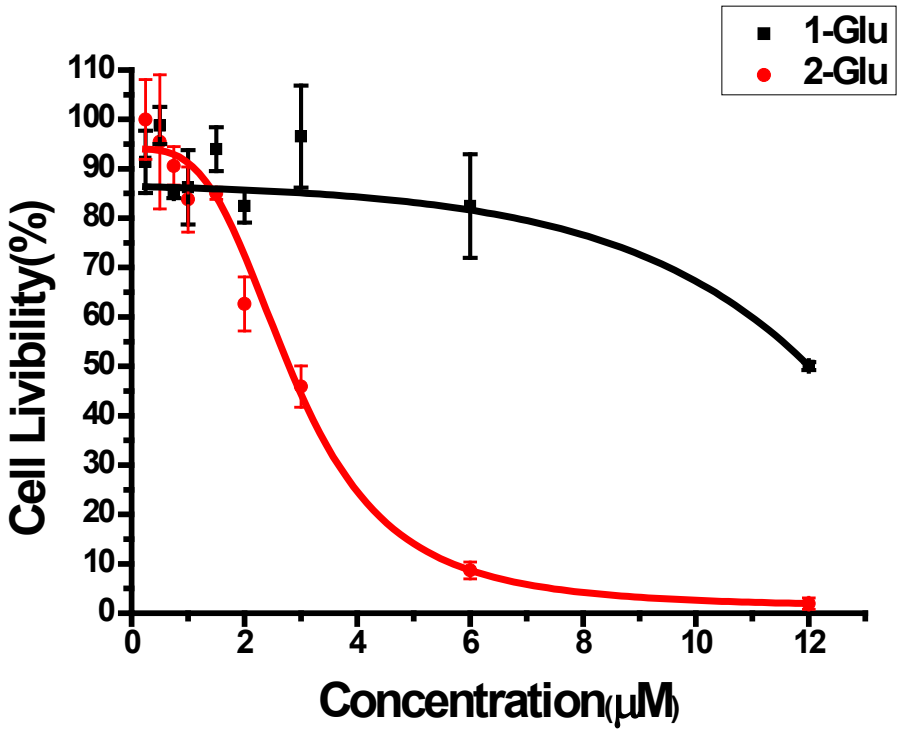

Figure S15 Light cytotoxicity of **1**-Glu and **2**-Glu toward Hela cells using CCK-8 assay. (Mean ±SD)

[a] Light source: visible light (400-700 nm, 6.5 w·cm^{-2}, 11.7 J·cm^{-2}).

[b] 24 h incubation in dark.

[c] Light source reported: 450 nm with CCK-8.

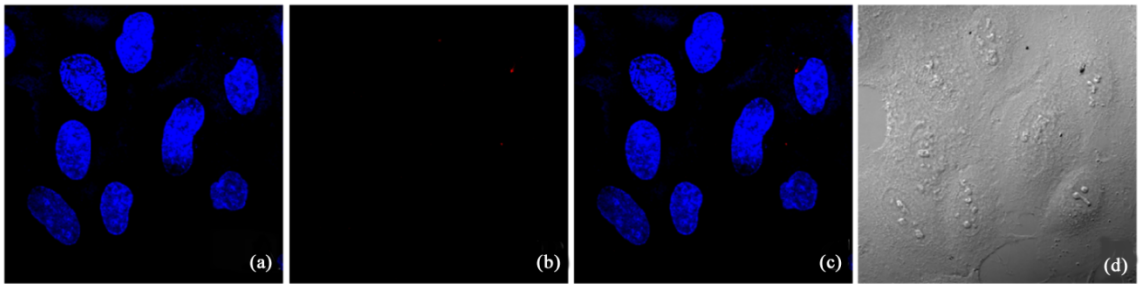

Figure S16 Photodynamic effect of **1**-Glu towards Hela cells viewed by confocal images. Hela cells were incubated with 1% DMSO for 24 h and then treated with light (585 nm, 2.72 $mW \cdot cm^{-2}$, 1.6 $J \cdot cm^{-2}$) for 10 min. (a) image of nuclei stained with Hoechst 33342, (b) the fluorescence image of DMSO, (c) merged images of (a) and (b). (d) DIC image which shows the cellular morphology.

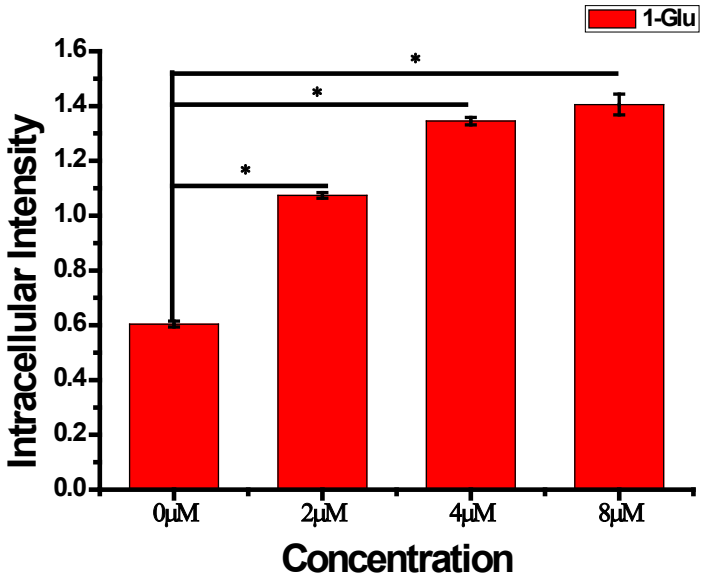

Figure S17 Intracellular ROS generation with **1**-Glu under different concentrations. 0 μM **1**-Glu is set as control. The significance of the differences between the mean values is demonstrated by $p < 0.001$ ($n = 30$) and marked by *. (Mean ±SD)

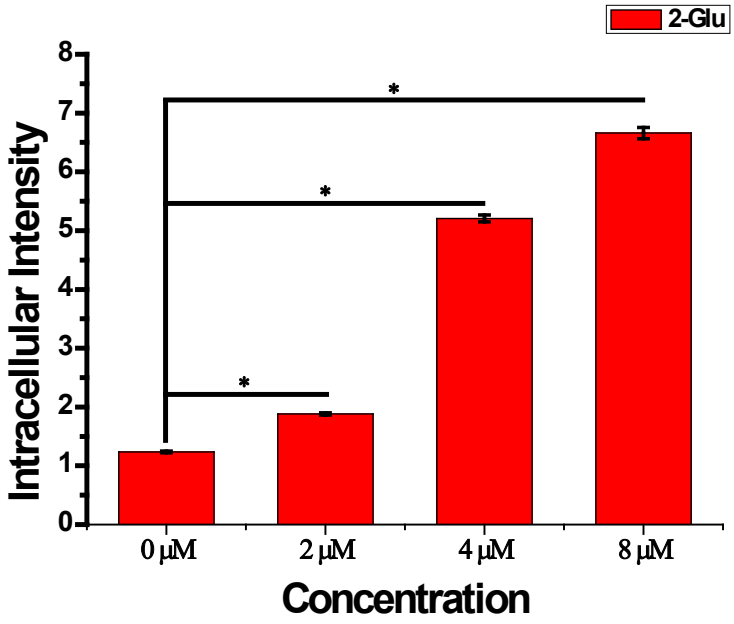

Figure S18 Intracellular ROS generation with **2**-Glu under different concentrations. 0 μM **2**-Glu is set as control. The significance of the differences between the mean values was demonstrated by $p < 0.001$ ($n = 30$) and marked by *. (Mean ±SD)

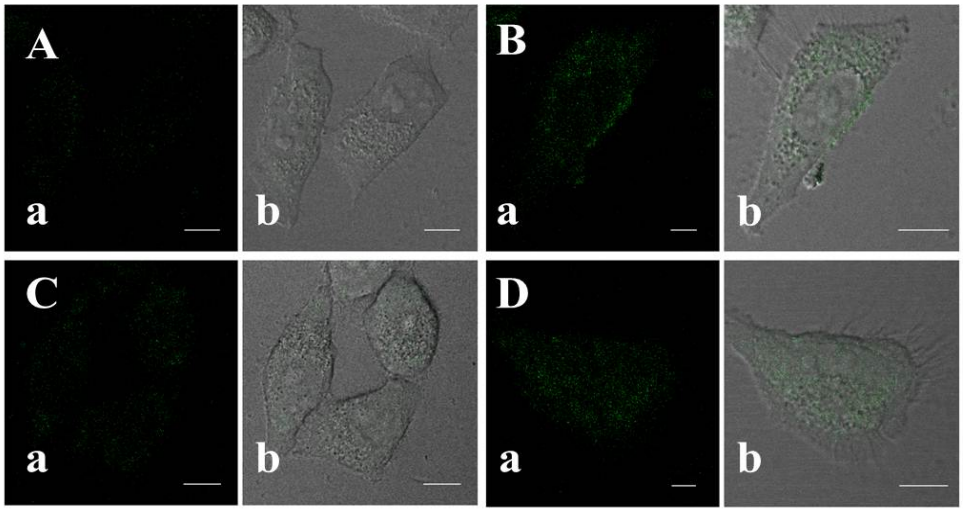

Figure S19 Confocal images of Hela cells under different concentrations of **1**-Glu for 30 min. (A) 0 μM; (B) 2 μM; (C) 4 μM;(D) 8 μM. (a) image of H2DCFDA; (b) merged image of (a) and Differential interference contrast (DIC) image.

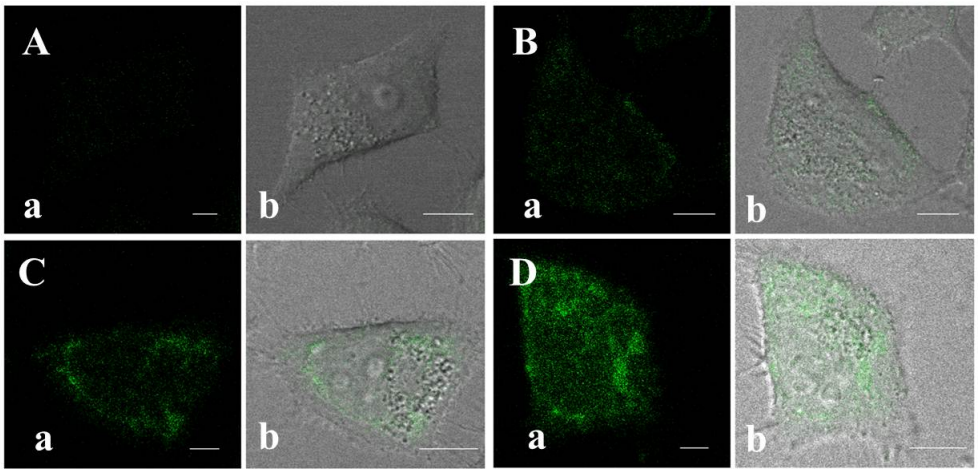

Figure S19 Confocal images of Hela cells under different concentrations of **2**-Glu for 30 min.(A) 0 μM; (B) 2 μM; (C) 4 μM; (D) 8 μM. (a) image of H2DCFDA; (b) merged image of (a) and Differential interference contrast (DIC) image.

5. Reference

1. *M. Pineiro, A. L. Carvalho, M. M. Pereira, A. M. d. A. R. Gonsalves, L. G. Arnaut and S. J. Formosinho, Chem.-Eur. J., 1998, **4**, 2299-2307.*
2. *J. Sangster, ed., Octanol-Water Partition Coefficients: fundamentals and physical chemistry, John Wiley and Sons, Chichester/New York, 1997.*
3. *G. E. Khalil, P. Daddario, K. S. F. Lau, S. Imtiaz, M. King, M. Gouterman, A. Sidelev, N. Puran, M. Ghandehari and C. Bruckner, Analyst, 2010, **135**, 2125-2131.*
4. *P. K. Goldberg, T. J. Pundsack and K. E. Splan, J. Phys. Chem. A, 2011, **115**, 10452-10460.*
5. *W. Spiller, H. Kliesch, D. Wöhrle, S. Hackbarth, B. Röder and G. Schnurpfeil, J. Porphyrins Phthalocyanines, 1998, **2**, 145-158.*
6. *F. Wilkinson, W. P. Helman and A. B. Ross, J. Phys. Chem. Ref. Data, 1993, **22**, 113-113.*
7. *C.-M. Che, J.-L. Zhang and L.-R. Lin, Chem. Commun., 2002, **0**, 2556-2557.*
8. *H. Athar, N. Ahmad, S. Tayyab and M. A. Qasim, Int. J. Biol. Macromol., 1999, **25**, 353-358.*
9. *A. Kriško, I. Piantanida, M. Kveder, G. Pifat, A. Lee, J. Greilberger, D. Kipmen-Korgun and G. Jürgens, Biophy. Chem., 2006, **119**, 234-239.*
10. *J. L. Goldstein, S. K. Basu, G. Y. Brunschede and M. S. Brown, Cell, 1976, **7**, 85-95.*
11. *M. Brown and J. Goldstein, Science, 1986, **232**, 34-47.*
12. *J. W. Newland, N. A. Strockbine, S. F. Miller, A. D. O'Brien and R. K. Holmes, Science, 1985, **230**, 179-181.*
13. *Y. Tamura, Y. Sato, A. Akaike and H. Shiomi, Brain Res., 1992, **592**, 317-325.*
14. *S. Ali, C. LeBel and S. Bondy, Neurotoxicology, 1992, **13**, 637.*
15. *W. Jakubowski and G. Bartosz, Cell Biol. Int., 2000, **24**, 757-760.*
16. *X. Chen, L. Hui, D. A. Foster and C. M. Drain, Biochem., 2004, **43**, 10918-10929.*
17. *Y. Yu, H. Lv, X. Ke, B. Yang and J.-L. Zhang, Adv. Synth. Catal., 2012, **354**, 3509-3516.*

6. Characterization Spectra

6.1 ^{1}H NMR and ^{19}F NMR

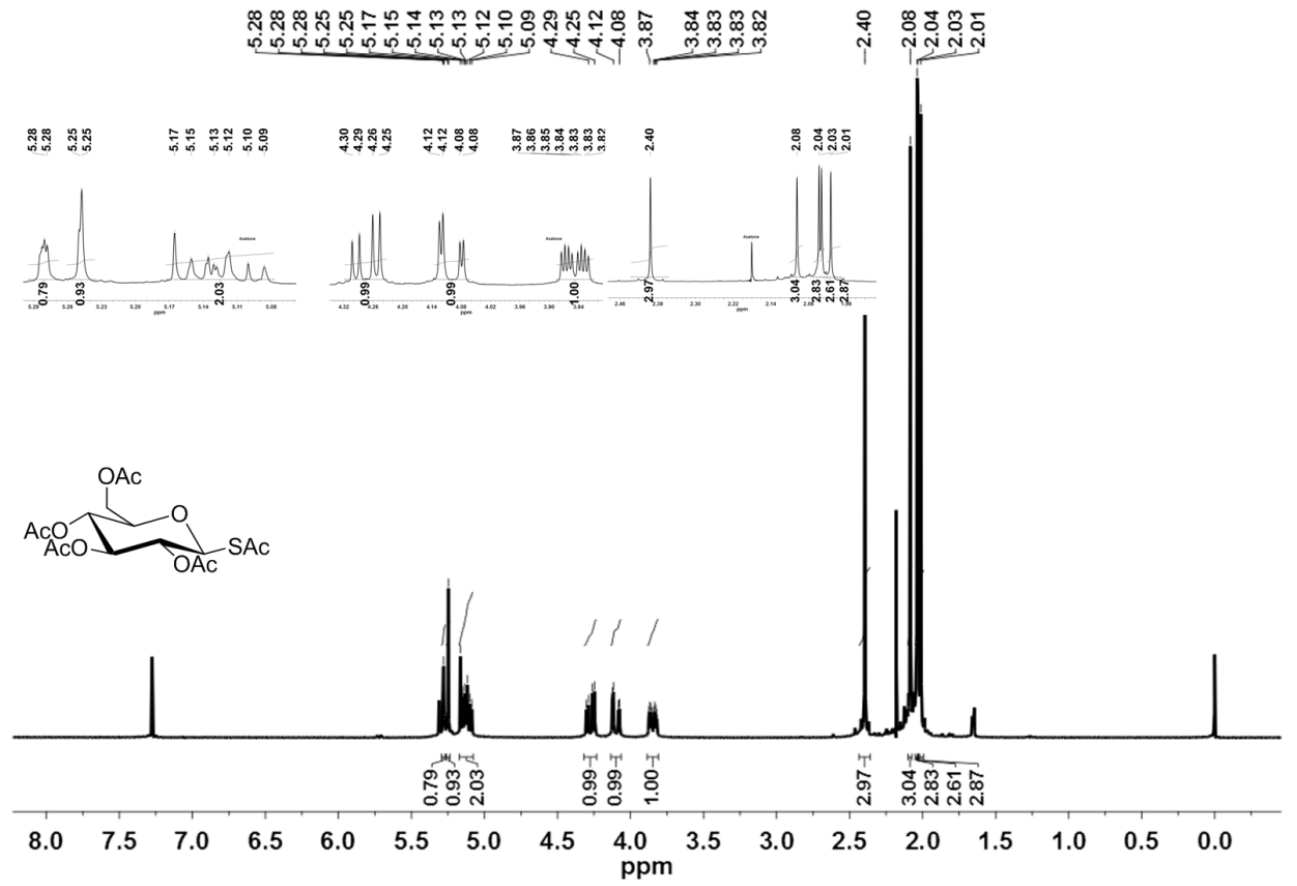

^{1}H NMR spectra of Glu(*O*Ac)$_4$-SAc in $CDCl_3$

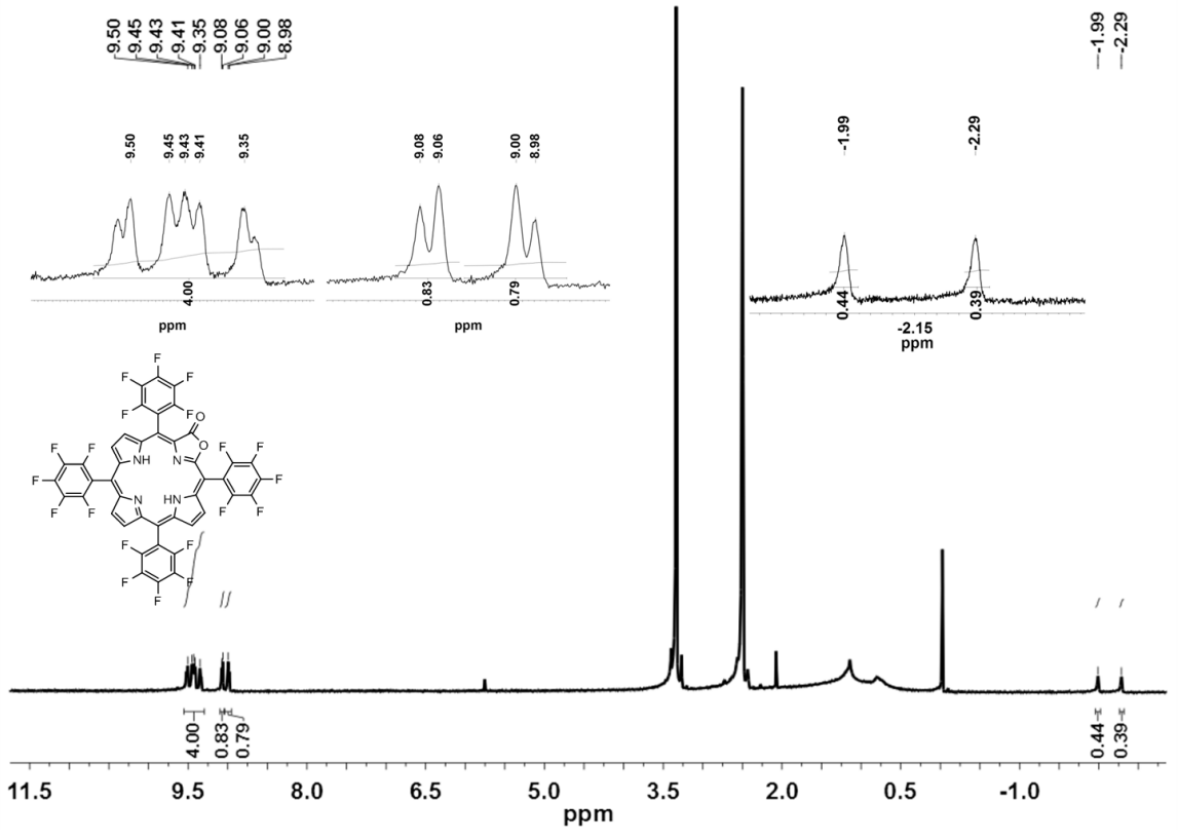

^{1}H NMR spectra of H_2F_{20}TPPL **(2)** in d^{6}-DMSO

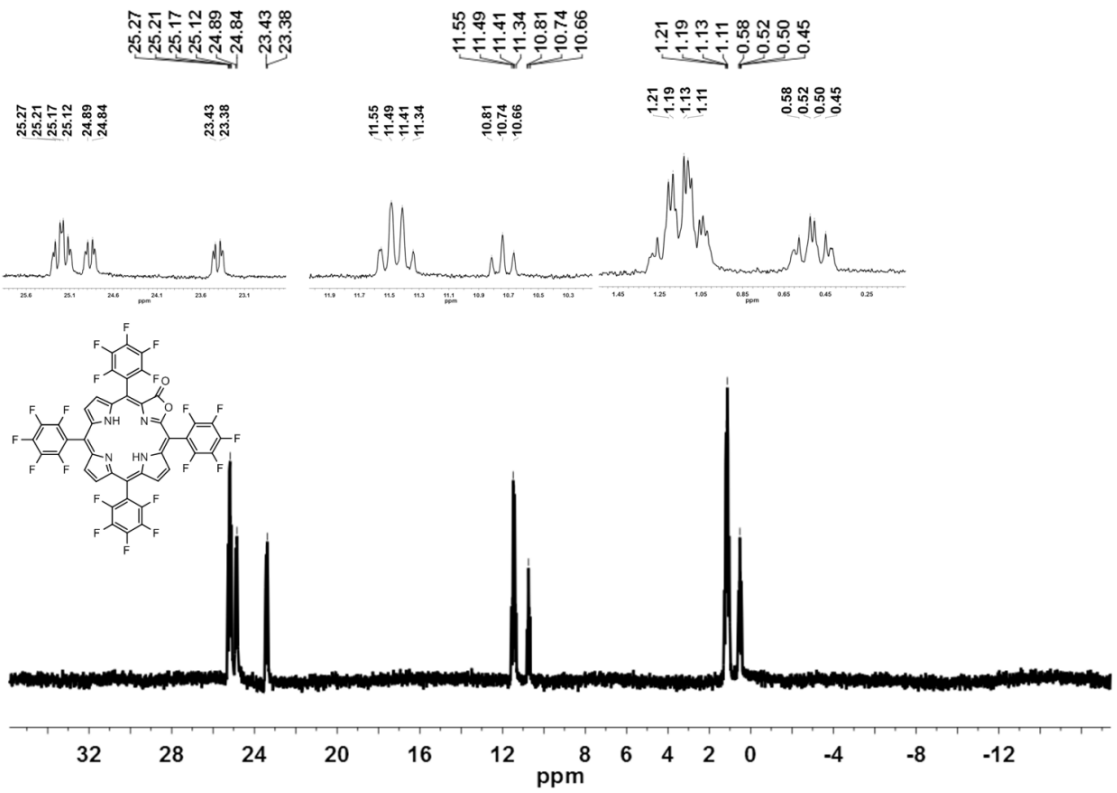

^{19}F NMR spectra of H_2F_{20}TPPL **(2)** in d^{6}-DMSO

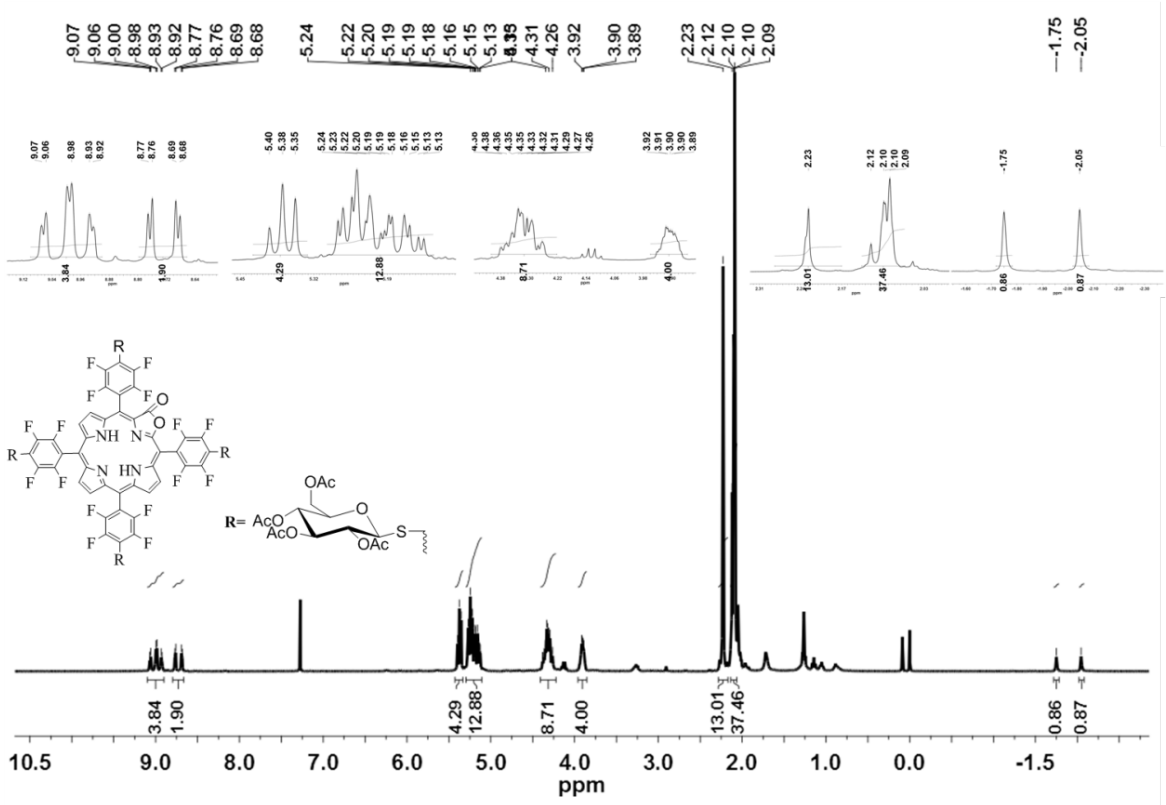

^{1}H NMR spectra of H_2F_{16}TPPL-S-Glu(*O*Ac)$_4$ in $CDCl_3$

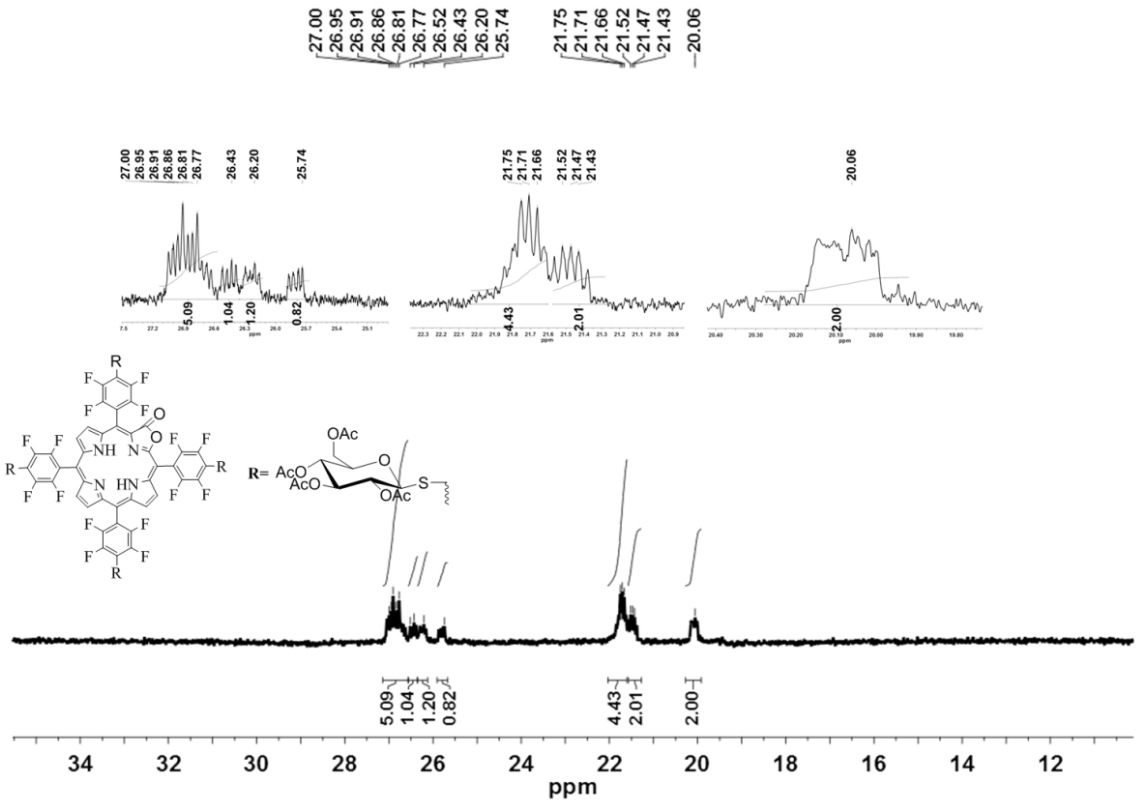

^{19}F NMR spectra of H_2F_{16}TPPL-S-Glu(*O*Ac)$_4$ in $CDCl_3$

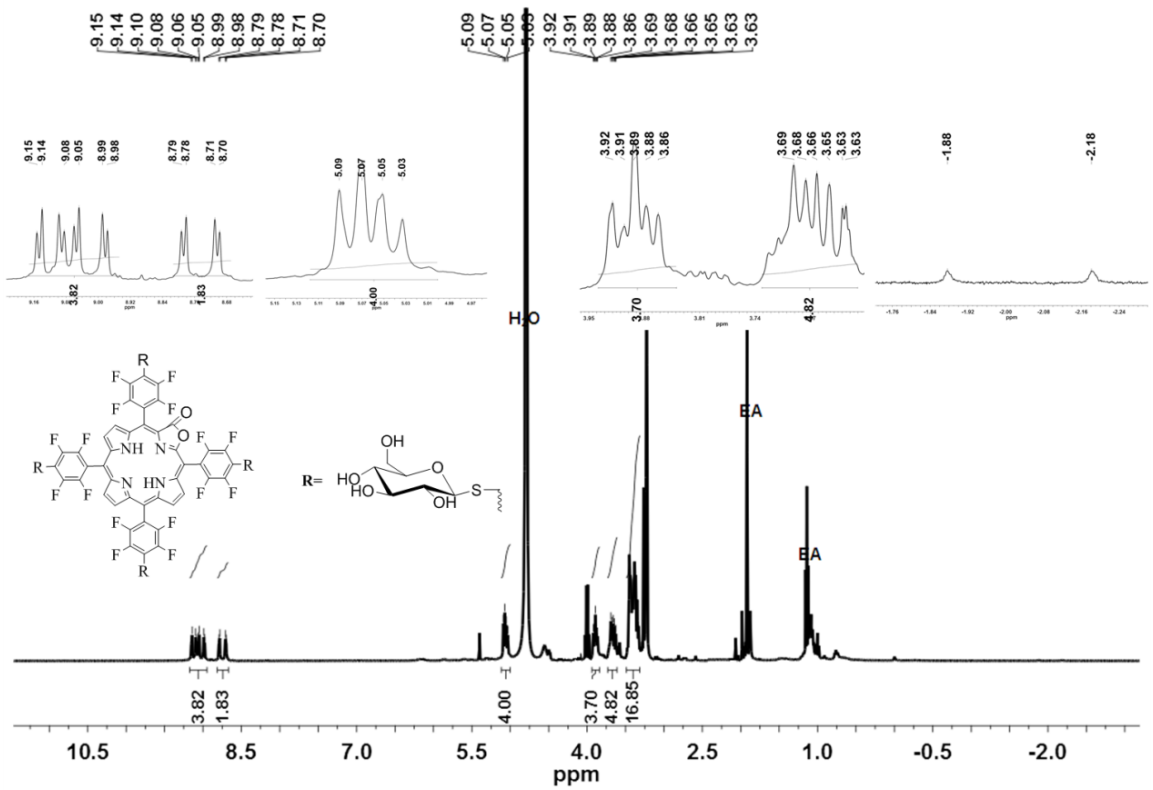

^{1}H NMR spectra of H_2F_{16}TPPL-S-GluOH$_4$ (**2**-Glu) in CD_3OD

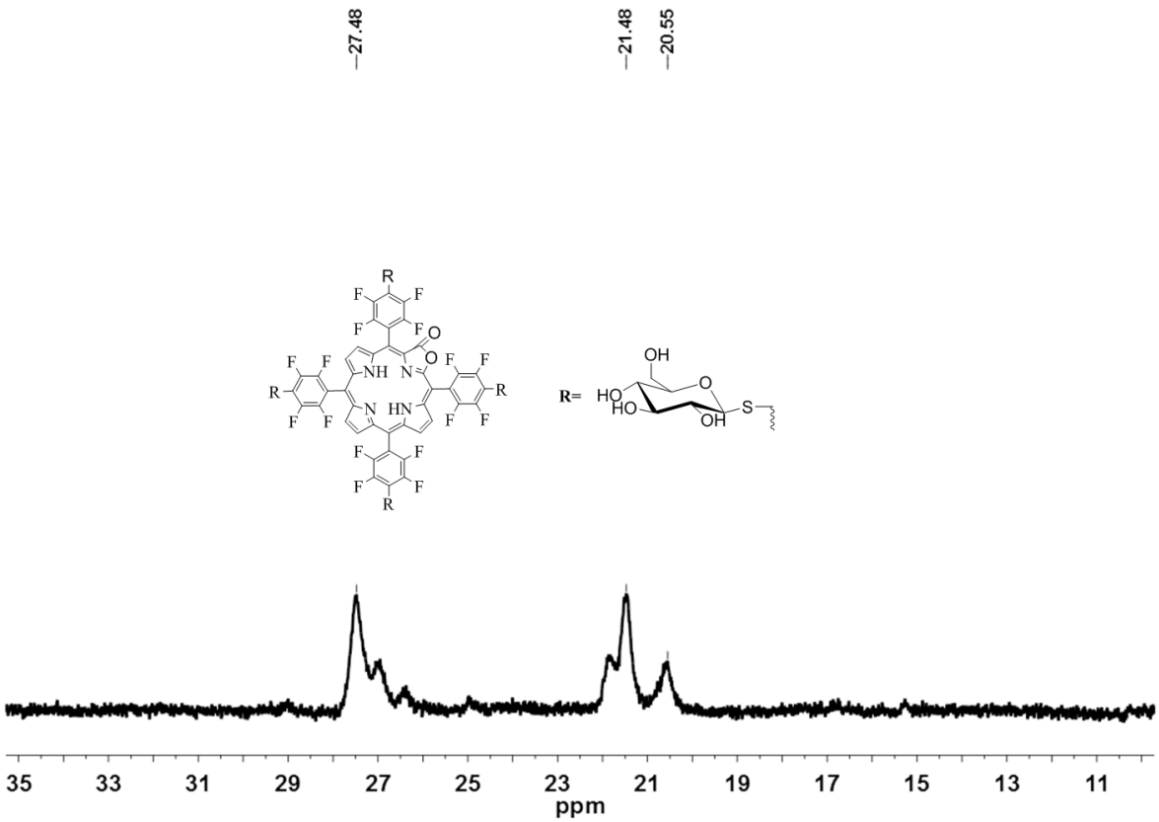

^{19}F NMR spectra of H_2F_{16}TPPL-S-GluOH$_4$ (**2**-Glu) in CD_3OD

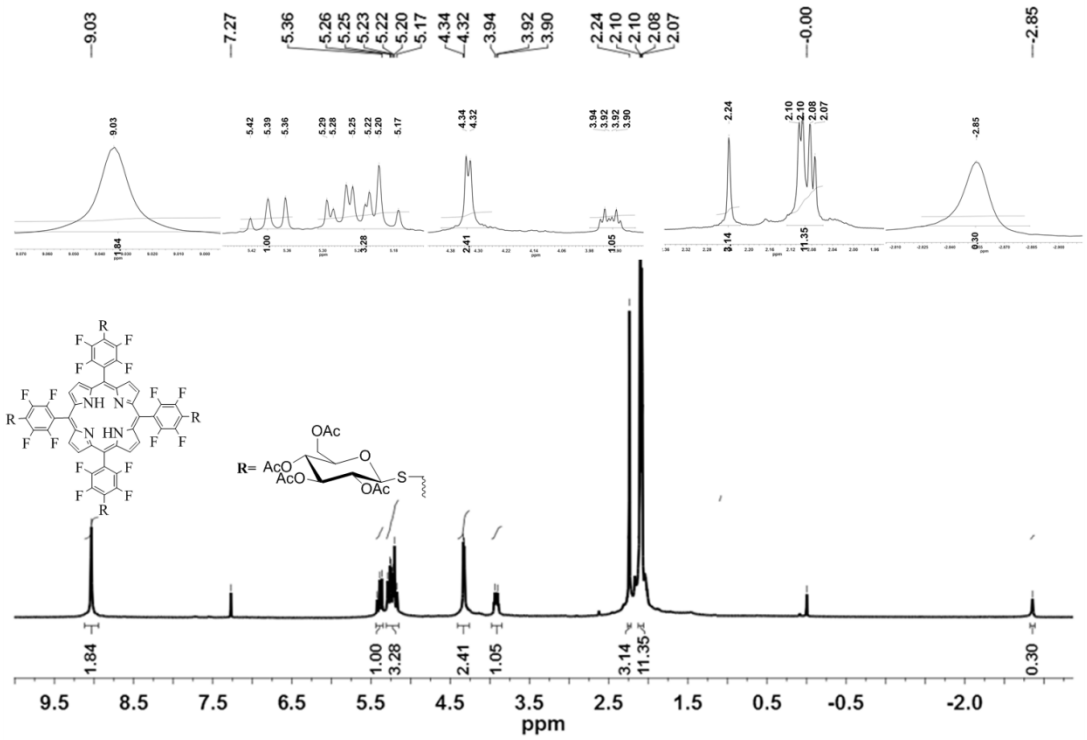

^{1}H NMR spectra of H_2F_{16}TPP-S-Glu(*O*Ac)$_4$ in $CDCl_3$

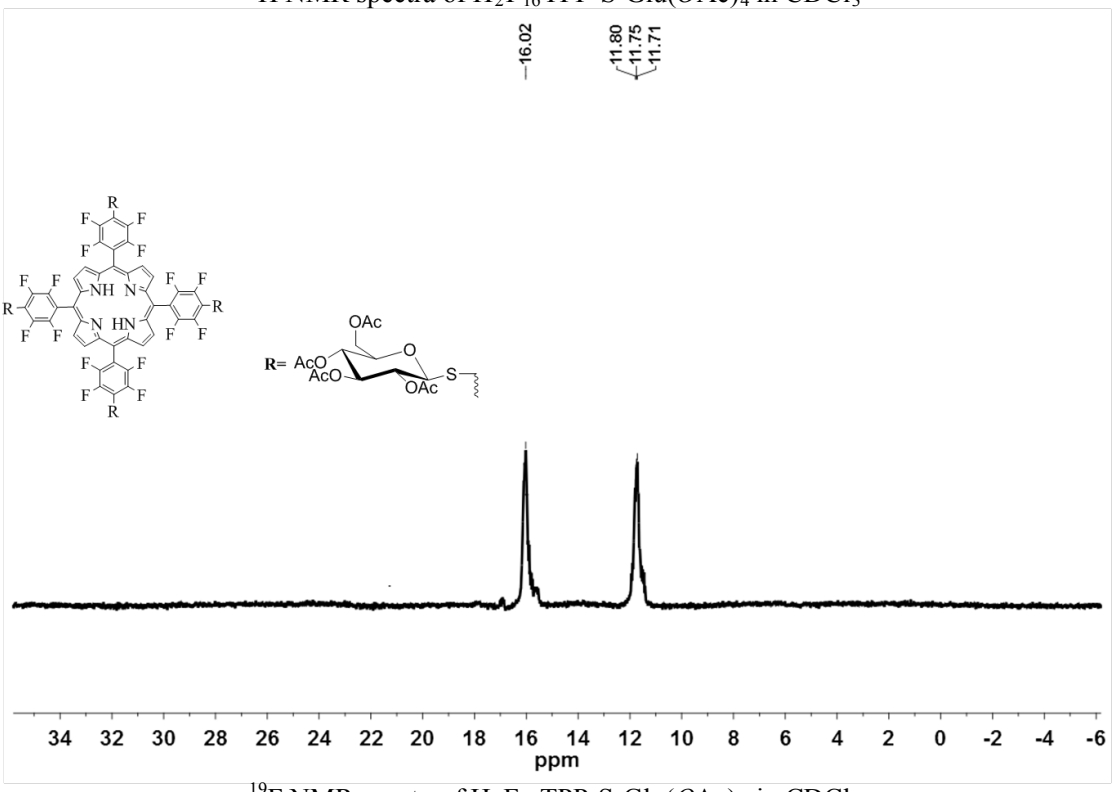

^{19}F NMR spectraof H_2F_{16}TPP-S-Glu(*O*Ac)$_4$ in $CDCl_3$

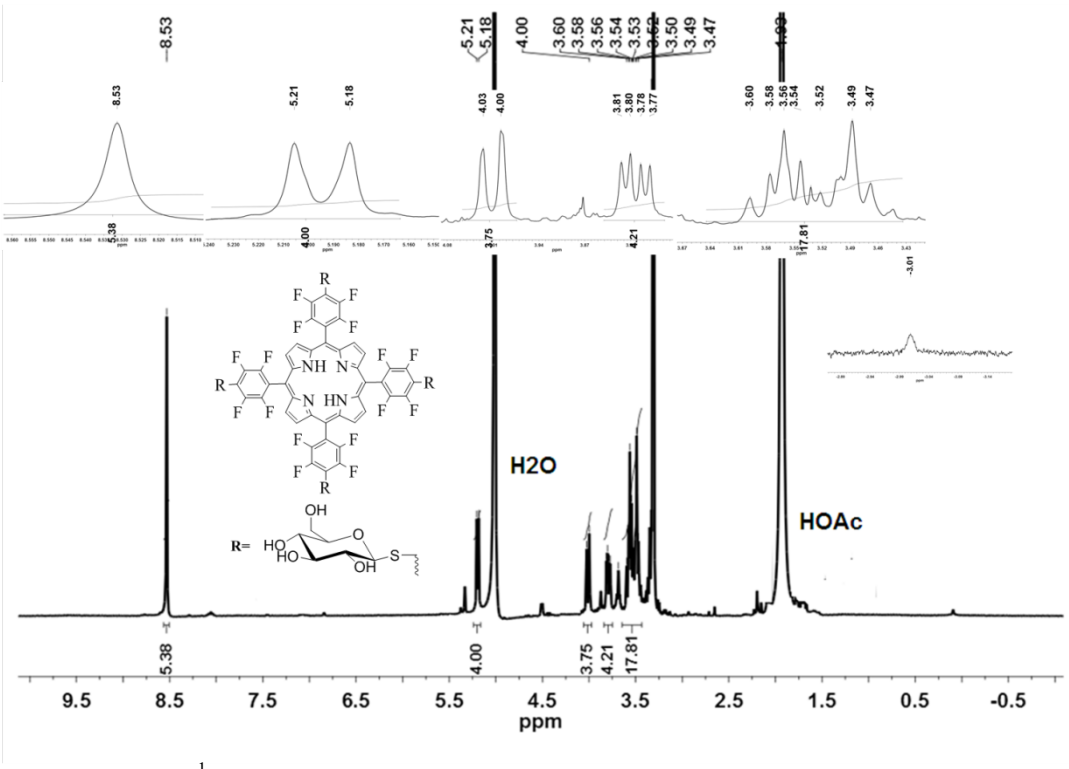

^{1}H NMR spectra of H_2F_{16}TPP-S-GluOH$_4$(**1**-Glu) in CD_3OD

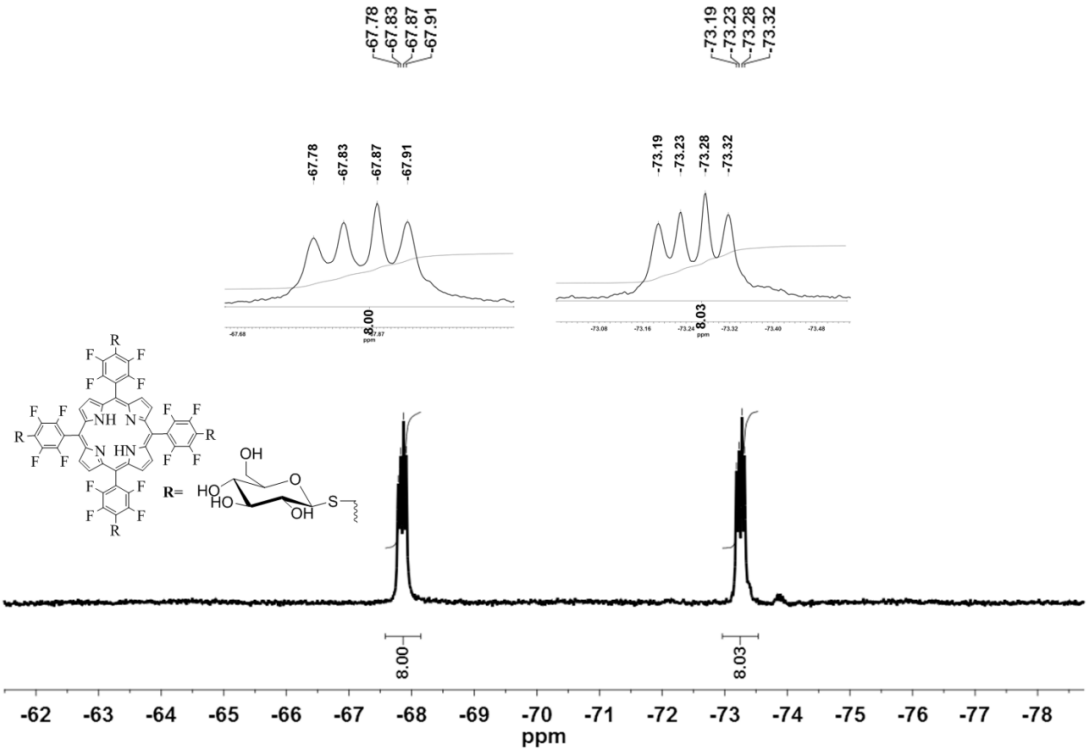

^{19}F NMR spectra of H_2F_{16}TPP-S-GluOH$_4$ (**1**-Glu) in CD_3OD

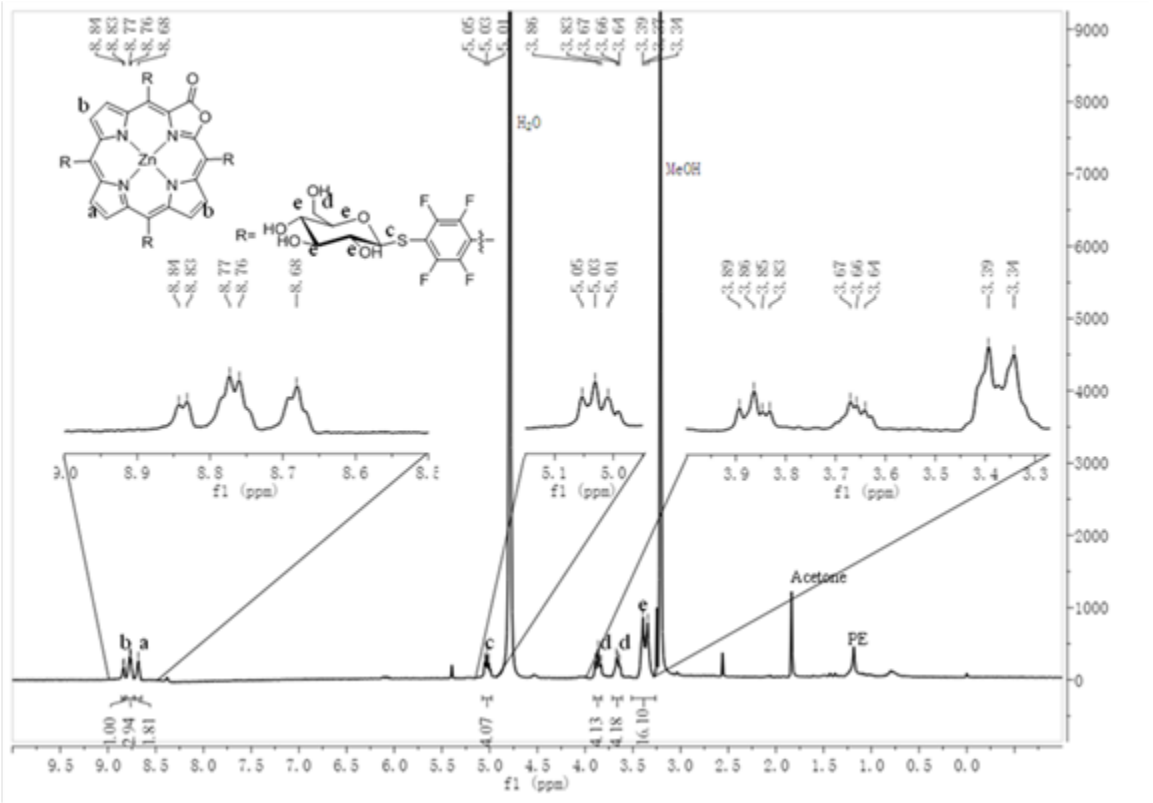

^{1}H NMR spectra of $ZnF_{16}TPPL\text{-}S\text{-}GluOH_4$ (**2**-ZnGlu) in CD_3OD

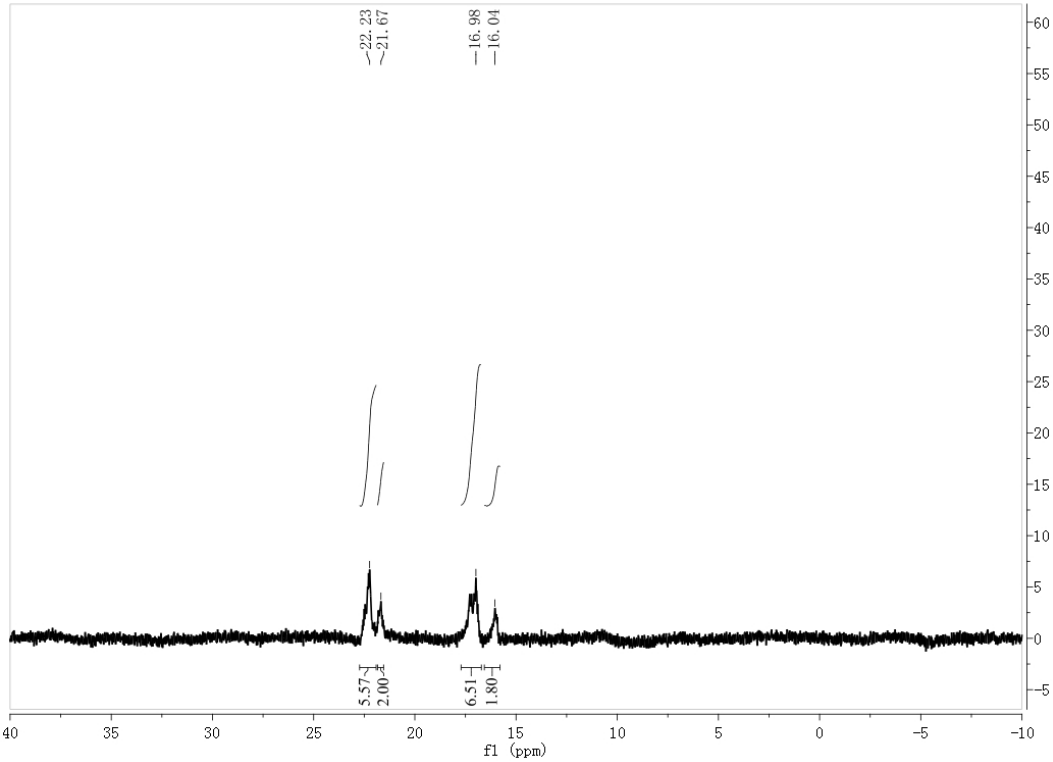

^{19}F NMR spectra of $ZnF_{16}TPPL\text{-}S\text{-}GluOH_4$ (**2**-ZnGlu) in CD_3OD

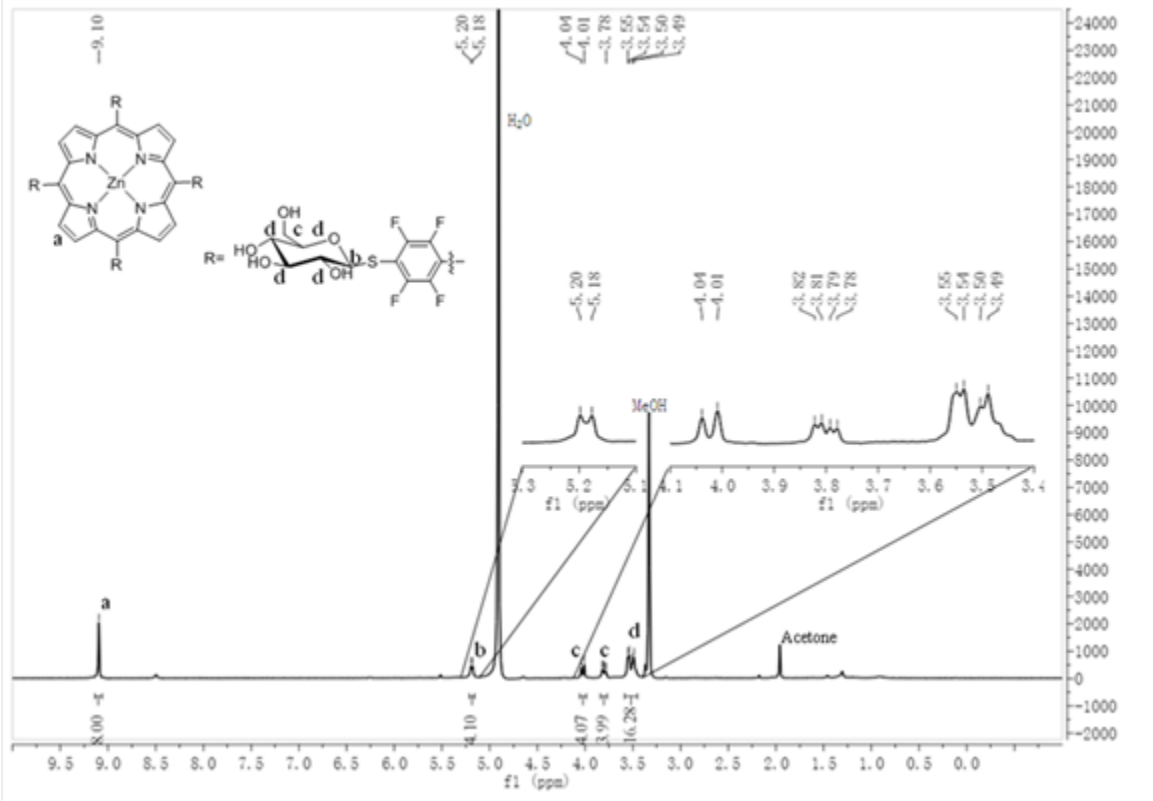

^{1}H NMR spectra of $ZnF_{16}TPP\text{-}S\text{-}GluOH_4$ (**1**-ZnGlu) in CD_3OD

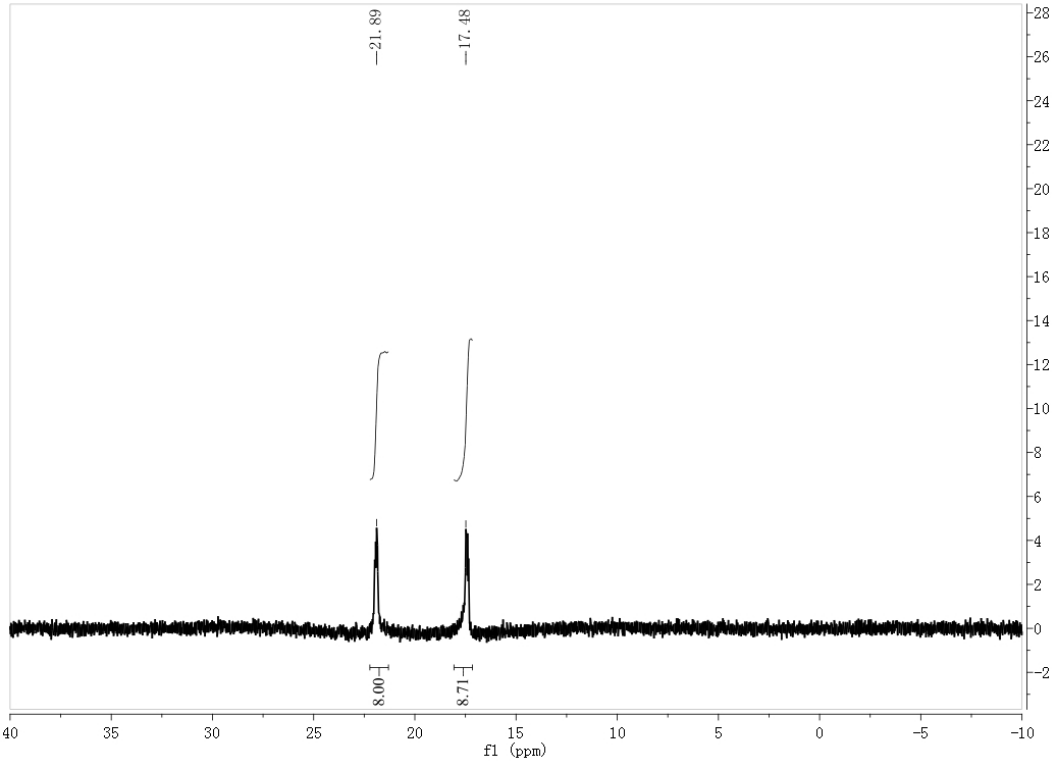

^{19}F NMR spectra of $ZnF_{16}TPP\text{-}S\text{-}GluOH_4$ (**1**-ZnGlu) in CD_3OD

6.2 MS spectra

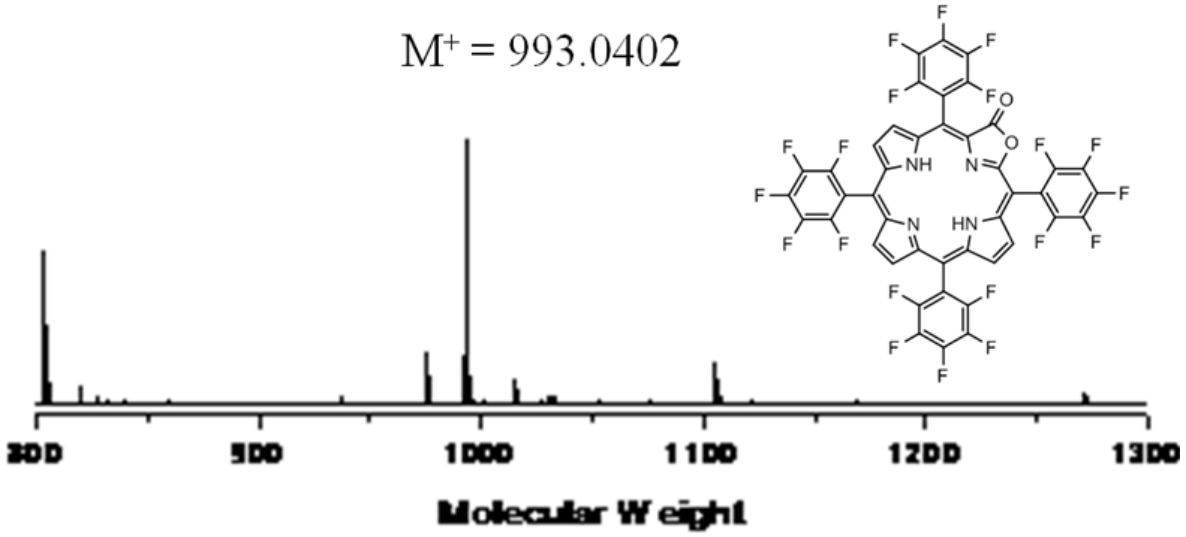

H_2F_{20}TPPL (**2**)

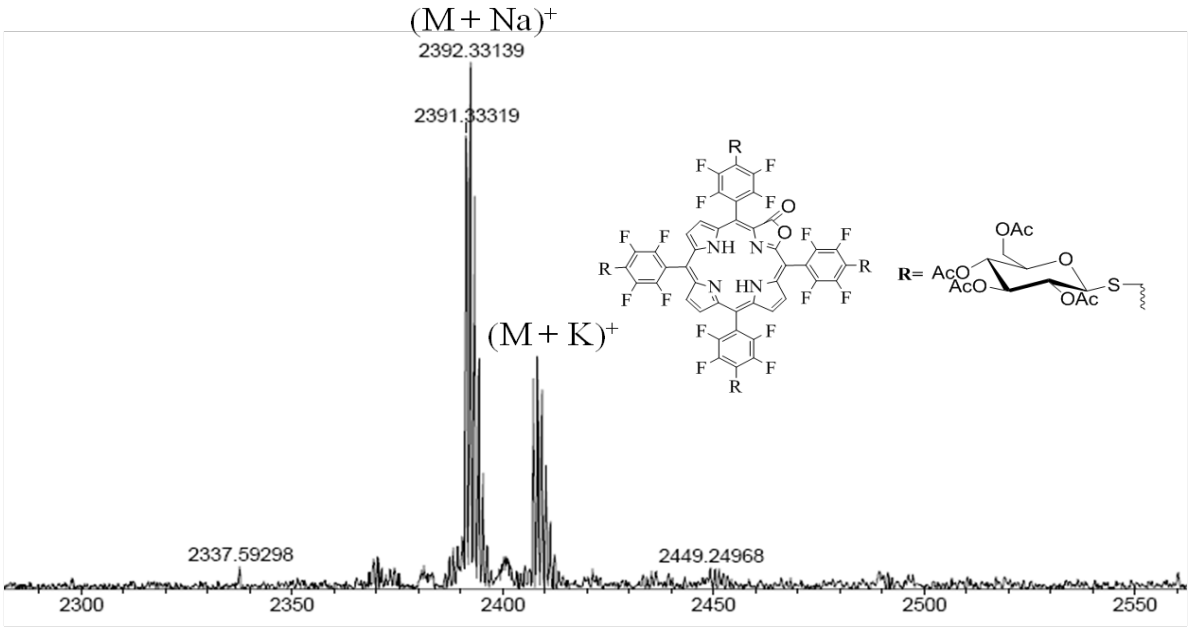

H_2F_{16}TPPL-S-Glu(*O*Ac)$_4$ (**2**-Glu(*O*Ac))

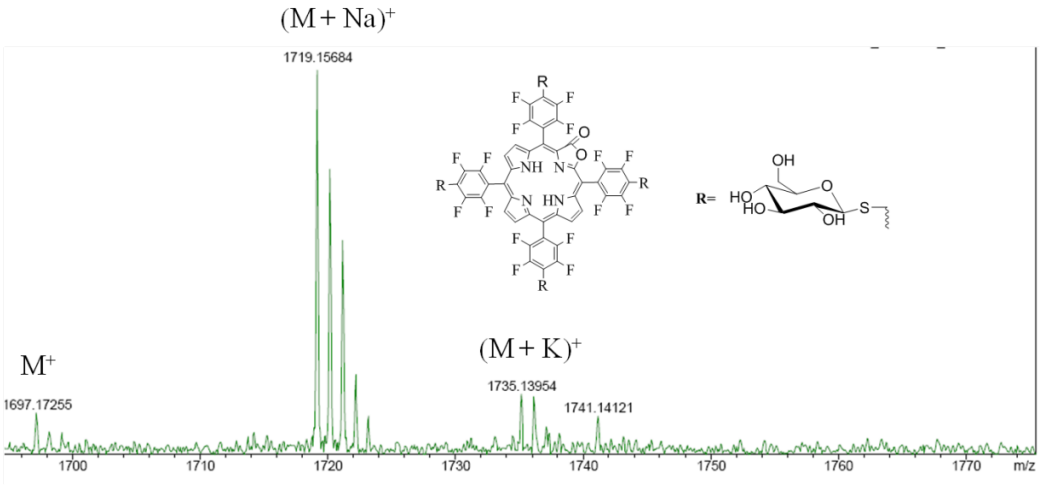

H_2F_{16}TPPL-S-GluOH$_4$ (**2**-Glu)

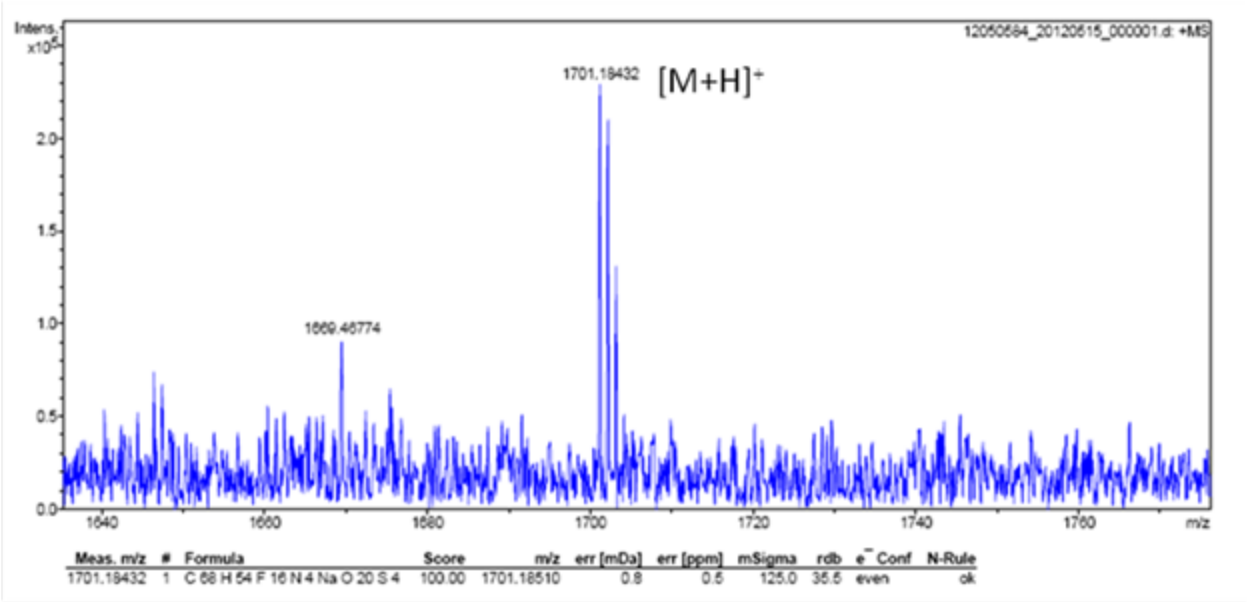

H_2F_{16}TPP-S-GluOH$_4$ (**1**-Glu)

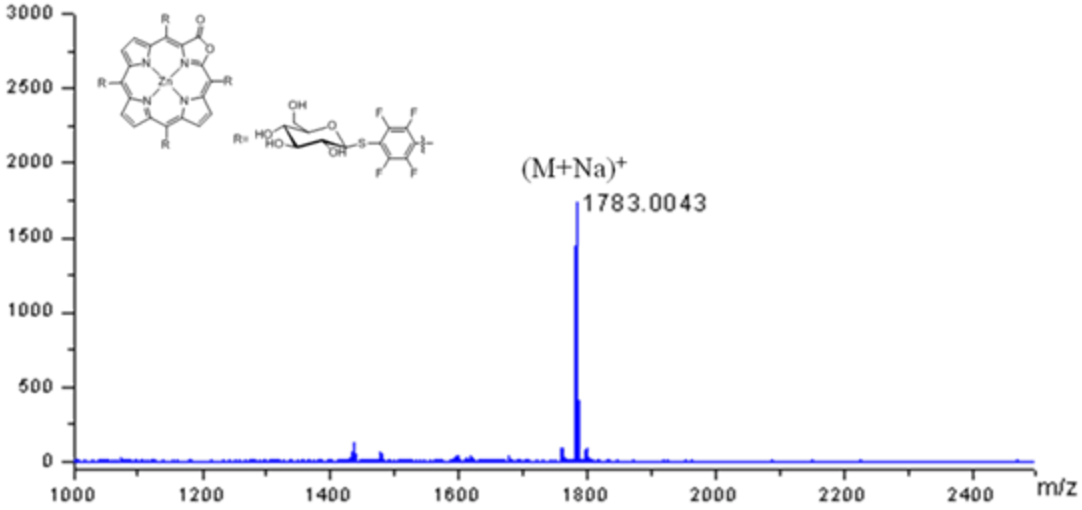

$ZnF_{16}TPPL\text{-}S\text{-}GluOH_4$ (**2**-ZnGlu)

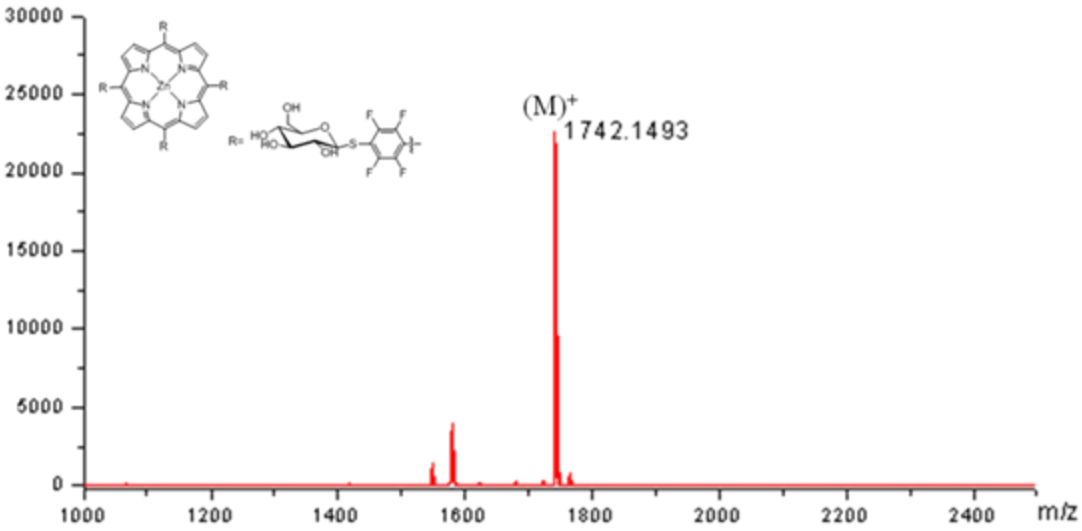

$ZnF_{16}TPP\text{-}S\text{-}GluOH_4$ (**1**-ZnGlu)

3.3 IR spectra

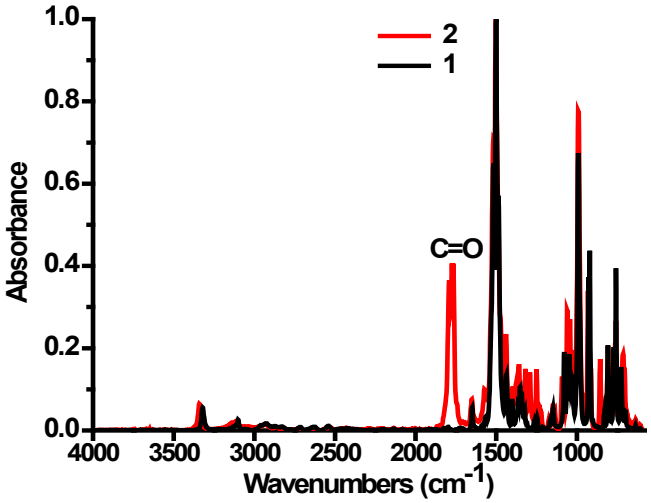

Infrared spectra of H_2F_{20}TPPL (**2**) and H_2F_{20}TPP (**1**), $\nu_{(C=O)}$ =1792, 1774, 1764 cm^{-1}.

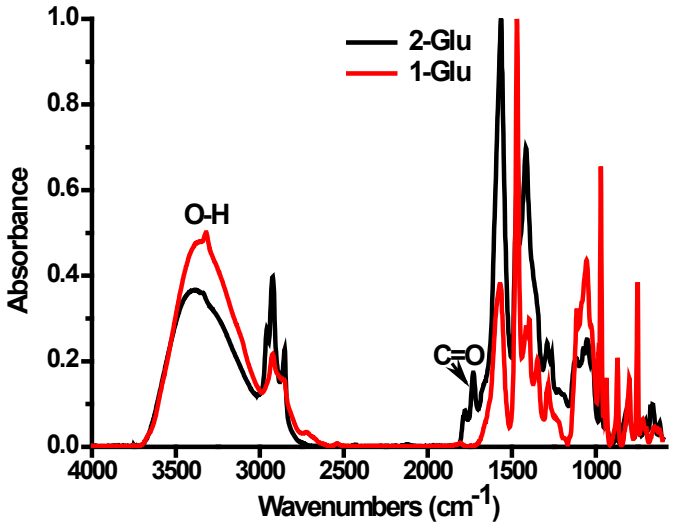

Infrared spectra of H_2F_{16}TPPL-S-GluOH_4 (**2**-Glu) and H_2F_{16}TPP-S-GluOH_4 (**1**-Glu), $\nu_{(O-H)}$ =3385 cm^{-1}, $\nu_{(C=O)}$ = 1728 cm^{-1}.

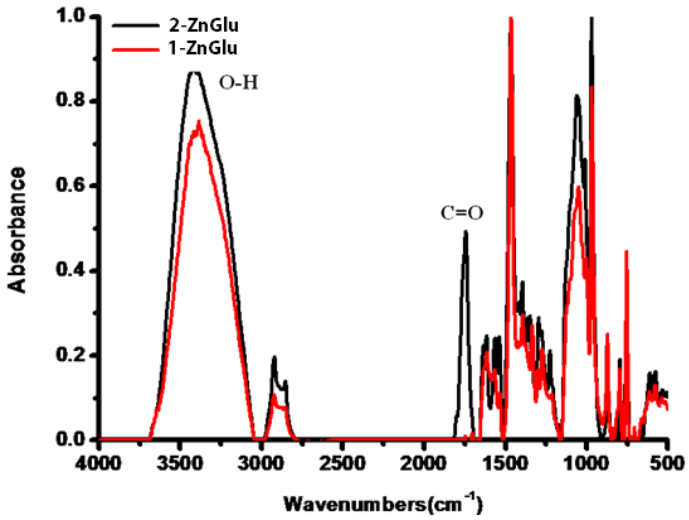

Infrared spects of ZnF_{16}TPPL-S-Glu (**2**-ZnGlu) and ZnF_{16}TPP-S-Glu (**1**-ZnGlu), $\nu_{(O-H)}$ =3385 cm^{-1}, $\nu_{(C=O)}$ =1745 cm^{-1}.